



**THESIS APPROVAL**  
**GRADUATE SCHOOL, KASETSART UNIVERSITY**

Master of Science (Chemistry)

DEGREE

Physical Chemistry

FIELD

Chemistry

DEPARTMENT

TITLE: Partial Oxidation of Methane on Transition Metals supported on HZSM-5 Zeolites

NAME: Miss Wayoon Wongpaiboonwatana

THIS THESIS HAS BEEN ACCEPTED BY

*Piboon Pantu*

THESIS ADVISOR

( Assistant Professor Piboon Pantu, Ph.D. )

*Supa Hannongbua*

COMMITTEE MEMBER

( Associate Professor Supa Hannongbua, Dr.rer.nat. )

*Cholticha Noomhorm*

COMMITTEE MEMBER

( Associate Professor Cholticha Noomhorm, Ph.D. )

*Yerry Mahatumarattana*

DEPARTMENT HEAD

( Assistant Professor Yerry Mahatumarattana, B.Sc. )

APPROVED BY THE GRADUATE SCHOOL ON 3 April 2006

*Vinai Arkongharn*

DEAN

( Associate Professor Vinai Arkongharn, M.A. )

# **THESIS**

## **PARTIAL OXIDATION OF METHANE ON TRANSITION METALS SUPPORTED ON HZSM-5 ZEOLITES**

**WAYOON WONGPAIBOONWATANA**

**A Thesis Submitted in Partial Fulfillment of  
the Requirements for the Degree of  
Master of Science (Chemistry)  
Graduate School, Kasetsart University  
2006**

**ISBN 974-16-1398-9**

Wayoon Wongpaiboonwatana 2006: Partial Oxidation of Methane on Transition Metals supported on HZSM-5 zeolites. Master of Science (Chemistry), Major Field: Physical Chemistry, Department of Chemistry. Thesis Advisor: Assistant Professor Piboon Pantu, Ph.D. 69 pages.  
ISBN 974-16-1398-9

The catalytic performance of various transition metals (with Fe, V, and Mo) supported on HZSM-5 zeolite for partial oxidation of methane by nitrous oxide at low reaction temperature has been investigated in a fixed-bed continuous flow reactor. The samples were characterized by XRF, ICP-AES, FTIR, N<sub>2</sub>-adsorption and H<sub>2</sub>-TPR. The major products for the reactions were carbon oxides but the formation of benzene and toluene as mirror products were also observed. The transition metals loading on HZSM-5 improved the activity for methane partial oxidation to higher hydrocarbons at 500°C. Formation rate of toluene was higher than benzene formation suggesting that these catalysts were active for methylation of benzene. The benzene and toluene formation increased with decreased Si/Al ratio while the ratios of CH<sub>4</sub>/N<sub>2</sub>O = 2 in feed gas were optimized for highest the yield of aromatics. However, the catalysts suffered severe coke formation and were deactivated within several minutes. The steam treatment slightly improved the deactivation time. When operating in pulse mode, it was clearly observed that benzene was formed before toluene and the conversion of methane and the selectivity to aromatics were rather stable and only a small amount coke deposited was occurred.

Wayoon Wongpaiboonwatana  
Student's signature

Piboon Pantu. 20 / 03 / 06  
Thesis Advisor's signature

## ACKNOWLEDGEMENTS

I would like to thank to a number of people who giving me the guidance, help and support to reach my goal of this thesis. First of all, most of credits in this thesis should justifiably go to my advisor, Assist. Prof. Dr. Piboon Pantu, for kindness, encouragement, guidance, and expert advice through all stages of this research. Appreciation is also extended to Assoc. Prof. Dr. Supa Hannongbua, Assoc. Prof. Dr. Cholticha Noomhorm and Assoc. Prof. Dr. Phungphai Phanawadee for their valuable assistance and all of my teachers, Prof. Dr. Jumras Limtrakul, Dr. Pensri Bunsawansong and Dr. Chak Sangma.

It is a pleasure to thank Assist. Prof. Dr. Tawan Sooknoi, Miss Suratsawadee Suwannaran, and Mr. Artit Ausavasukhi from King Mongkut's Institute of technology Ladkrabang (KMITL) for their help with XRF analysis.

I would like to acknowledge financial supports from the Higher Education Development Project Scholarship (MUA-ADB funds), Kasetsart University Research and Development Institute (KURDI) and Graduated School, Kasetsart University (Thesis and Dissertation Support Fund to W.W.)

Deep appreciation are due to Mrs. Wilasinee Wongpaiboonwatana, my mother who lives in heaven now, my family and all of my friends to give me sincerity and make me happy.

Wayoon Wongpaiboonwatana

February 2006

## TABLE OF CONTENTS

	<b>Page</b>
TABLE OF CONTENTS.....	i
LIST OF TABLES.....	iii
LIST OF FIGURES .....	iv
LIST OF ABBREVIATIONS .....	vi
INTRODUCTION .....	1
LITERATURE REVIEWS .....	3
MATERIALS AND METHODS.....	17
Materials .....	17
Major equipments.....	17
Chemicals.....	17
Experimental Methods .....	18
Preparation of Catalysts.....	18
Characterization of catalysts.....	19
Catalytic activity testing.....	20
Calculation Methods.....	22
RESULTS AND DISCUSSION .....	23
Characterization of catalysts.....	23
Catalytic Activity.....	30
CONCLUSION .....	43
LITERATURE CITED .....	44

**TABLE OF CONTENTS (Cont'd)**

	<b>Page</b>
APPENDIX.....	50
Appendix A: Calibration Method and Calculation method.....	51
Appendix B: Oral Presentation.....	56

## LIST OF TABLES

Table		Page
1	Elemental analysis results for all samples by XRF and ICP-AES techniques.....	23
2	BET Surface Areas and Micropore Volumes of the transition metals supported HZSM-5 catalysts.....	24
3	Summarized FTIR spectra of modified and unmodified HZSM-5 zeolites.....	27
4	Catalytic performance of various catalysts at 500°C in the feed gas 10%CH <sub>4</sub> : 10%N <sub>2</sub> O: 2%H <sub>2</sub> and flow rate 100 ml/min.....	31
5	Effect of the ratio of CH <sub>4</sub> /N <sub>2</sub> O on the catalytic performance in the presence of H <sub>2</sub> at 500°C.....	34
6	Effect of Si/Al ratio on the catalytic performance of catalysts in methane aromatization in the presence of H <sub>2</sub> at 500°C.....	36
7	BET Surface Areas and Micropore Volumes of steamed and unsteamed catalysts.....	39
8	Effect of the steam treatment on methane aromatization in the feed 10%CH <sub>4</sub> :5%N <sub>2</sub> O:2%H <sub>2</sub> at 500°C with flow rate 100 ml/min.....	40
 <b>Appendix Table</b>		
A1	Summarized of relative response factor of gases.....	54

## LIST OF FIGURES

Figure	Page
1 Experimental setup.....	22
2 Normalized FTIR spectra of the OH stretching region of HZSM-5 and Fe/HZSM-5 samples heated at 400°C for 1.5h: (a) SH27; (b) impFe/SH27; (c) Ex-Fe/SH27; (d) SH55; (e) Ex-Fe/SH55.....	25
3 Normalized FTIR spectra of the OH stretching region of HZSM-5 and V/HZSM-5 samples heated at 400°C for 1.5h: (a) SH27; (b) impV/SH27; (c) Ex-V/SH27; (d) SH55; (e) Ex-V/SH55.....	26
4 Normalized FTIR spectra of the OH stretching region of HZSM-5 and Mo/HZSM-5 samples heated at 400°C for 1.5h: (a) SH27; (b) imp2%Mo/SH27; (c) Ex-Mo/SH27; (d) SH55; (e) impMo/SH55.....	26
5 Temperature programmed reduction profiles of Fe/HZSM-5 zeolite: (a) impFe/SH27; (b) Ex-Fe/SH27; (c) Ex-Fe/SH55.....	28
6 Temperature programmed reduction profiles of V/HZSM-5 zeolite: (a) impV/SH27; (b) Ex-V/SH27; (c) Ex-V/SH55.....	28
7 Temperature programmed reduction profiles of Mo/HZSM-5 zeolites: (a) impMo/SH27; (b) Ex-Mo/SH27; (c) impMo/SH55.....	29
8 The %conversion of methane and nitrous oxide and % selectivity of products of catalyst at 500°C in the feed gas 10%CH <sub>4</sub> : 10%N <sub>2</sub> O: 2%H <sub>2</sub> and flow rate 100 ml/min: (a) Ex-V/SH27, (b) Ex-Fe/SH27, (c) impMo/SH27 .....	32
9 Effect of the ratio of CH <sub>4</sub> /N <sub>2</sub> O on the catalytic performance in the presence of H <sub>2</sub> at 500°C: (a) %CH <sub>4</sub> conversion; (b) %selectivity of aromatics; (d) %yield of aromatics.....	35
10 Effect of Si/Al ratio on the catalytic performance of catalysts in methane aromatization in the feed 10%Ar:10%CH <sub>4</sub> :5%N <sub>2</sub> O:2%H <sub>2</sub> at 500°C.....	36



## LIST OF FIGURES (cont'd)

Figure	Page
11 The %conversion of methane and % selectivity of products of catalyst at 500°C in the feed gas 10%CH <sub>4</sub> : 5%N <sub>2</sub> O: 2%H <sub>2</sub> and flow rate 100 ml/min: (a) SH27; (b) Ex-Fe/SH27.....	37
12 Normalized FTIR spectra of the OH stretching region of samples heated at 400°C for 1.5h: (a) Ex-V/SH55; (b) Ex-Fe/SH55; (c) steam Ex-V/SH55; (d) steam Ex-Fe/SH55.....	38
13 Pulse reaction on Ex-Fe/SH27 catalysts at 500°C: (a) catalytic activity; (b) MS signal .....	41
 <b>Appendix Figure</b>	
A1 Calibration curves of (a) CH <sub>4</sub> and (b) Ar.....	53
B1 Transient reaction of 4 wt % Mo/H-ZSM5 with methane.....	59
B2 Bifunctional Mechanism.....	60
B3 Thermodynamic limit of direct conversion of CH <sub>4</sub> under nonoxidative conditions.....	60
B4 Catalytic performance of various catalysts at 450°C.....	63
B5 Pulse reaction on 2%wt Mo/HZSM-5 catalysts.....	64
B6 Effect of H <sub>2</sub> addition to pulse reaction on 2%wt Mo/HZSM-5 catalysts with and without H <sub>2</sub> at 500°C.....	65
B7 Effect of CH <sub>4</sub> :N <sub>2</sub> O ratio on 2%wt Mo/HZSM-5 catalysts without H <sub>2</sub> at 500°C: CH <sub>4</sub> :N <sub>2</sub> O = 1 and CH <sub>4</sub> :N <sub>2</sub> O = 2.....	66
B8 Formation rate of benzene and toluene and CH <sub>4</sub> conversion on 2%wt Mo/HZSM-5 catalysts at 500°C.....	67

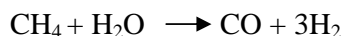
## LIST OF ABBREVIATIONS

ASAP	=	Accelerated Surface Area and Porosimetry Analyzer
BET	=	Brunauer Emmett Teller
EPR	=	Electron Paramagnetic Resonance
EXAFS	=	Extended X-ray Absorption Fine Structure
FTIR	=	Fourier-Transform Infrared Spectroscopy
GC	=	Gas Chromatography
ICP-AES	=	Inductively Coupled Plasma-Atomic Emission Spectrometry
MAS-NMR	=	Magic Angle Spinning Nuclear Magnetic Resonance
MCM	=	Mobile Crystalline Material
MDA	=	Methane Dehydroaromatization
MS	=	Mass Spectroscopy
NMR	=	Nuclear Magnetic Resonance
SAPO	=	Silica Aluminophosphates
SEM	=	Scanning Electron Microscopy
SH27	=	HZSM-5 SiO <sub>2</sub> /Al <sub>2</sub> O <sub>3</sub> =27
SH55	=	HZSM-5 SiO <sub>2</sub> /Al <sub>2</sub> O <sub>3</sub> =55
TCD	=	Thermal Conductivity Detector
TG	=	Thermalgravimetric analysis
TM	=	Transition Metal
TPCO <sub>2</sub>	=	CO <sub>2</sub> -Temperature Programmed Reaction
TPD	=	Temperature Programmed Desorption
TPO	=	Temperature Programmed Oxidation
TPR	=	Temperature Programmed Reduction
UV-VIS	=	Ultra Violet-Visible Spectroscopy
XAS	=	X-ray Absorption
XRD	=	X-ray Diffraction
XRF	=	X-ray Fluorescence Spectroscopy
XPS	=	X-ray Photoelectron Spectroscopy
ZSM-5	=	Zeolite Socony Mobil 5

# **PARTIAL OXIDATION OF METHANE ON TRANSITION METALS SUPPORTED ON HZSM-5 ZEOLITES**

## **INTRODUCTION**

Conversion of methane, the main component of the natural gas, to partial oxidized products, or higher hydrocarbons and aromatics has received great attention due to a strong economic incentive for better utilization of the abundant natural gas reserves worldwide. A number of strategies have been explored and developed methods at levels that range from fundamental science to engineering technology for the conversion of methane. This conversion can be divided into two groups, direct and indirect methods. The direct method includes (a) the synthesis of methanol and formaldehyde, (b) oxidative coupling of methane to ethylene and (c) conversion of methane to aromatics and hydrogen in the absence of oxygen. The indirect conversion mainly relies on the production of synthesis gas; a mixture of hydrogen and carbon oxides, which can be used for the synthesis of methanol, dimethyl ether, gasoline and production of hydrocarbons and higher alcohols via the Fischer-Tropsch synthesis (Lunsford, 2000). Due to the highly endothermic nature of the steam reforming reaction is a major route methane conversion to synthesis gas.



The formation of synthesis gas has large energy consumption and a high operating cost. Therefore, an alternative route of the direct conversion is more desirable and very challenging.

However the reaction usually is carried out at rather high temperatures (900-1200K) due to the activation of the first C-H bond is the most difficult, while products are more readily oxidized to carbon oxides resulting in low selectivity and/or low yield of products. Approaches to overcome these problems are preventing further oxidation of the interested products, e.g., the high temperature non-oxidative activation of light alkanes, and the search for new activation process.

Recently, The methane dehydroaromatization (MDA) to aromatics in the absence of an oxidant at high temperature (973-1023K) has been widely studied on transition metals (Mo, Fe, V, W, and Cr)/HZSM-5 zeolites. The molecular shape selectivity of the zeolite channels remarkably affects the product distribution of the reaction (Weckhuysen *et al.*, 1998 and Ichikawa *et al.*, 1997). Silica-alumina-type zeolites with a two-dimensional structure and a pore size near the dynamic diameter of benzene such as HZSM-5, HMCM-22, and HZSM-11 zeolites are good catalysts for MDA. The interaction between active metals and the Brønsted acid sites of the zeolite is very important for the preparation of a good catalyst (Shu *et al.*, 2001). The major problems are catalyst deactivation, and low aromatic yield. The major challenge for this methane conversion is to reach higher yields of higher hydrocarbon products, in particular, the alkylation of aromatic hydrocarbons such as toluene, ethylbenzene, and xylenes, and branched aliphatic compounds while also operate at a lower temperature.

Using an alternative oxidizing agent such as nitrous oxide has shown to increase activity and selectivity to the partial oxidation products. For example, Fe/ZSM-5 can activate methane at room temperature and partially oxidize it to methanol by using nitrous oxide as an oxidant (Knops-Gerrits *et al.*, 2001). The reactive oxygen radical derived from nitrous oxide decomposition may enhance methane activation and reduce the reaction temperature. The activated methane can undergo oxidation reactions or dehydroaromatization to aromatics or higher hydrocarbons. The transition metals supported zeolite catalyst can act as bifunctional catalyst where both metal and acidic site play two different roles in the reaction. The pore structure of ZSM-5 zeolite is suitable for formation of aromatic benzene. In this research, the partial oxidation of methane on the transition metal supported on zeolites was investigated with the emphasized on the formation of higher hydrocarbon products at low reaction temperature.

## LITERATURE REVIEWS

### 1. Methane dehydroaromaization of methane

Transformation of methane to aromatics is thermodynamically more favorable than the transformation of methane to ethylene, extensive have devoted to the direct conversion in heterogeneous catalysis. In 1983, Shepelev *et al.* reported that trace aromatics could be detected in the reaction of methane with oxygen or nitric oxide over ZSM-5 and HZSM-5 zeolites, but the main products would be CO<sub>2</sub>, CO and H<sub>2</sub>O. The formation of oxygen containing products provides a thermodynamic driving force so that the reaction has a negative free energy. Therefore, the reaction of methane with oxygen to form carbon oxides and water is thermodynamically much more favorable than the direct conversion of methane into aromatics.

### 2. Modified of HZSM-5 catalysts and optimization of reaction condition

Many researchers have investigated in order to improve the catalytic activity, selectivity and stability of the products as summarized in the term of the role of zeolite micropores and metallic sites. Recently, the methane dehydroaromatization to aromatics with Mo/HZSM-5 has been focused on zeolite supported catalyst. In addition, the preparation method, calcinations temperature can affect the catalytic performance. Optimization of reaction condition has also been studied in the different reaction conditions, such as pretreatment, reaction temperature, pressure, and space velocity, etc.

In 1998, Zhang *et al.* found that the catalytic performance of Mo-based catalysts supported on various zeolites for methane aromatization in the absence of oxygen in a fixed-bed continuous-flow quartz reactor, and their catalytic properties were correlated with features of zeolite structure. They examined H-type silica–alumina zeolites, such as ZSM-5, ZSM-8, and ZSM-11. Among of them, they found that MoO<sub>3</sub>/HZSM-11 had the best activity and stability. The catalytic performance of

MoO<sub>3</sub>/HZSM-8 was lower than MoO<sub>3</sub>/HZSM-5, while activity of MoO<sub>3</sub>/H-BETA was lower than MoO<sub>3</sub>/HZSM-8. Catalysts supported on H-MCM-41 and H-SAPO-34 exhibited low activity for methane aromatization and those supported on H-MOR, H-X and H-Y gave only a little amount of ethylene. Over MoO<sub>3</sub>/H-SAPO-5 and MoO<sub>3</sub>/H-SAPO-11 no hydrocarbons were detected. While in 2004, D.Y. Wang *et al.* investigated nanosize MCM-49 zeolite was synthesized by the hydrothermal method, and it was used as the support of MoO<sub>3</sub>/zeolite catalysts for methane aromatization in the absence of oxidant under various reaction conditions. After the preparation method of catalysts and reaction conditions were optimized, high benzene selectivity of around 90% were obtained with a yield of more than 10% at 973K over the 6 wt. % Mo/HMCM-49 catalyst and the catalyst could keep the activity for more than 150 h. Compared to Mo/HZSM-5 catalysts, Mo/HMCM-49 was easier to prepare and more effective. They considered that the excellent catalytic performance of Mo/HMCM-49 catalyst for methane aromatization.

Shu *et al.* (2003) investigated a novel Re/HMCM-22 for the methane dehydrocondensation reaction towards benzene and naphthalene. Re/HMCM-22 was similarly active and selective catalyst for the reaction as Mo/HZSM-5, Re/HZSM-5 and Mo/HMCM-22 catalysts. The catalytic performances of HMCM-22 supported rhenium and molybdenum catalysts were higher benzene selectivity and lower naphthalene selectivity as well as of higher catalytic stability than those of HZSM-5 supported catalysts. The differences of channel structures of HMCM-22 and HZSM-5 supported catalysts related to their catalytic behavior, where HMCM-22 has large cavities and slit-like pore openings. The catalytic stabilities of both catalysts were improved greatly by the addition of a few percent of carbon dioxide in methane feed and the pre-dealumination of HMCM-22 and HZSM-5 supports by acid-reflux.

However, many researchers confirmed that the HZSM-5 is the best support for methane dehydroaromatizaion. In 1995, Chen *et al.* examined the conversion of methane over Mo/HZSM-5 catalysts with different molybdenum loading. The influence of reaction temperature and the space velocity of methane were observed. The both of surface areas and the pore volumes decreased with increasing amount of

molybdenum. The effect of calcinations on the catalyst structure was the redispersion of the Mo species, which led to the change in the chemical environment of molybdenum atoms into the channels of HZSM-5 zeolite. The dehydro-oligomerization of methane in the absence of oxidant increased methane conversion after the introduction of molybdenum to the HZSM-5 zeolite. But more addition of molybdenum resulted in decreasing of the activity and selectivity to benzene. It was found that the catalyst with molybdenum loading 2-3 wt% exhibited optimum activity for the dehydro-oligomerization of methane to aromatics. The methane oligomerization reaction was proposed to be catalyzed by molybdenum species together with the Brønsted acid sites of HZSM-5 zeolite. Ethylene was a primary product while benzene was a final product of the reaction.

In 2002, Tan *et al.* investigated the effect of oxygen addition on methane dehydrogenation and aromatization over 2%wt Mo/HZSM-5. The rising of oxygen concentration decreased aromatics selectivity but increased in carbon monoxide selectivity. The addition of suitable amount of oxygen (5.3%vol) and NO (9.1%vol) was beneficial to the catalytic stability. During the oxidative reaction of methane, there were three reaction regions in the catalyst bed, which were methane oxidation, methane reforming, and methane aromatization. With the rising in oxygen or NO concentration, the aromatization region disappeared, while CO and CO<sub>2</sub> were the predominant carbon containing products.

In the same year, Tan *et al.* also studied the effect of calcinations temperature on the acidity of catalyst, the channel structure, and the states and location of Mo species in the HZSM-5. The calcinations at 500°C caused the Mo species disperse on the external surface and diffuse into the channels of the zeolite, while the calcinations of catalyst at high temperature caused in the deactivation for the methane aromatization reaction. The raising of the calcinations temperature from 500 to 750°C could deduce the polymeric Mo species dispersed on HZSM-5 in the form of small crystallites, surface area, pore volume and decrease in the amount of Brønsted acid sites. The results showed that at high temperature decreased the methane conversion and benzene selectivity but increased in C<sub>2</sub>-hydrocarbon yield.

In 2003, Wang *et al.* reported that post-steam-treatment improved the catalytic performances of Mo/HZSM-5 catalysts in methane dehydroaromatization under nonoxidative conditions. The treatment could enhance the stability of the catalyst and also give a higher methane conversion and a higher yield of light aromatics, as well as a decrease in the formation rate of carbonaceous deposits. However, a severe post-steam-treatment with longer treating time of the 6%Mo/HZSM-5 catalyst led to the formation of the  $\text{Al}_2(\text{MoO}_4)_3$  phases, which was destroyed to the reaction.

In 1998, Weckhuysen *et al.* discussed the conversion of methane to benzene in the absence of oxygen over different TM/HZSM-5 zeolites (with Mo, Fe, V, W, and Cr) as a function of the preparation and treatment method, the metal ion loading, and the zeolite acidity. Nonoxidative methane activation was characterized by an induction period prior to the formation of benzene, toluene, and naphthalene. During induction period, no hydrocarbon products were formed, and the major gas phase products were CO, CO<sub>2</sub>, and H<sub>2</sub>O. Optimum catalytic performance was obtained for 2–4 wt% TM/HZSM-5 zeolites with CO prereduced, and their activities decreased in the order: Mo>W>Fe>V>Cr. The catalytic performance was strongly dependent on the preparation method, the treatment condition, and the metal loading. The activity of catalysts prepared by impregnation was always higher than solid state ion exchanged materials. The differences in catalytic activity and selectivity between impregnated and solid state ion-exchanged materials can be explained in terms of differences in zeolite acidity and the state of the transition metal ion. The supported transition metal ions were predominantly located in the zeolite channels of solid state ion materials. For the impregnated samples, the transition metal ions were mainly located at the outer surface. And the induction period decreased with increasing time at moderate reduction temperature and with increasing metal oxide loading. The methane activation was influenced by catalyst prereduction, except for Fe/HZSM-5 prepared by impregnation. From above results, they showed that for methane dehydroaromatization the HZSM-5 zeolite is one of the best supports, and the best transition metals is Mo. So among all the investigated catalyst, Mo/HZSM-5 is the best catalyst.



The addition of a second metal component also influence on the catalytic performance of the Mo/HZSM-5 catalyst. In 1999, Ohnishi *et al.* studied the catalytic dehydroaromatization of methane performed by the addition of CO and CO<sub>2</sub> at 1 atm and 973 K on Mo/HZSM-5 and Fe/Co-modified Mo/HZSM-5. The addition of a few percent of CO and CO<sub>2</sub> to methane feed promotes benzene production and significantly improves the stability of the Mo/HZSM-5 catalyst at prolonged times-on-stream. For Fe- and Co-modified Mo/HZSM-5 catalysts the methane reaction with CO yields higher activities of benzene production with good catalytic stability for more than 100 h due to the coke formation to less than 20%. TPO experiments revealed that the amount of coke formed on the catalyst surface was greatly reduced by adding a few percent of CO or CO<sub>2</sub> to the methane feed gas and also reduced the reactive coke by addition of CO<sub>2</sub> more than 4%. The role of CO addition to methane feed is based on the formation of amounts of CO<sub>2</sub> and carbon, where carbon was hydrogenated to an active carbon species (CH<sub>x</sub>) involving methane conversion toward aromatic products such as benzene and naphthalene, while CO<sub>2</sub> reacted with the surface inert carbon deposit to regenerate CO, resulting in improving catalyst stability due to efficient suppression of coke formation on the catalyst.

In 2001, Tang *et al.* studied the effect of Si/Al ratio of HZSM-5, pretreatment and additives on catalytic activity of nonoxidative conversion of methane to aromatics over impregnated Mo/HZSM-5 catalysts. The Si/Al ratio of HZSM-5 zeolites had an important effect on the yields of benzene and toluene, while the HZSM-5 with low Si/Al ratio had more methane conversion and benzene selectivity than high Si/Al ratio. It was also found that the effect between Co promotion and HCl acidified pretreatment was exhibited in the 3%Mo-1%Co-HCl/HZSM-5, which Co additive was beneficial to the cracking of methane and the formation of CH<sub>x</sub> species and HCl acidified pretreatment may increase the surface acid site. Mo<sub>2</sub>C was the only detected surface molybdenum species after exposure to methane.

### 3. The study of active phase of methane dehydroaromatization

Now a day, the detail of mechanism of the intermediate and structure of active species remain unclear. In 1995, Chen *et al.* studied the structures of catalysts were characterized and a possible mechanism of methane transformation under nonoxidizing conditions over Mo/HZSM-5 catalyst was also proposed. The predominant molybdenum species was heptamolybdate ions in solution with the pH value of the impregnating solution at about 6. From the infrared spectra, it was apparent that the  $917\text{ cm}^{-1}$  band most probably resulted from the heptamolybdate species. The molybdenum oxide species are not easily reduced because of the strong oxide support interaction. Therefore, the maximum reduction temperatures in the TPR profiles of catalyst increased with an increase in molybdenum content.

In 1997, Wang *et al.* investigated carbon deposits of the dehydroaromatization of methane to benzene over a 2 wt% Mo/ZSM-5 catalyst in the absence of an added oxidant. The reaction was investigated by an induction period, prior to the initiation of benzene production, during which  $\text{Mo}_2\text{C}$  was formed and coke deposition occurred. The formation of the carbide was confirmed by X-ray photoelectron spectroscopy (XPS) measurements. Pretreatment of the catalyst in a  $\text{CH}_4/\text{H}_2$  gas mixture at  $700^\circ\text{C}$  reduced  $\text{Mo}^{6+}$  ions in the calcined catalyst into  $\text{Mo}_2\text{C}$  and almost eliminated the induction period, confirming that  $\text{Mo}_2\text{C}$  was the active species in the activation of methane. Under typical  $\text{CH}_4$  reaction conditions at  $700^\circ\text{C}$ , the original  $\text{Mo}^{6+}$  ions could reduce to form  $\text{Mo}_2\text{C}$ , with the remaining Mo occurring primarily as  $\text{Mo}^{4+}$  and traces of  $\text{Mo}^{5+}$  ions. These non-reducible Mo ions were most likely within the channels of the zeolite. XPS, ion scattering spectroscopy, and FTIR measurements indicate that Mo species in a Mo/ZSM-5 sample dried at  $130^\circ\text{C}$  are present as small crystallites of the original ammonium heptamolybdate impregnated salt on the external surface of the zeolite. After calcinations at higher temperatures ( $500\text{--}700^\circ\text{C}$ ), Mo becomes more highly dispersed, but not uniformly distributed, on the external surface of the zeolite. During preparation and pretreatment of the catalyst, a part of the Mo ions diffused into the channels of the zeolite. The amount of Mo ions in the channels depended on the temperature, time, and atmosphere of

calcinations. The roles of  $\text{Mo}_2\text{C}$ , partially reduced Mo ions, and the origin of the induction period were discussed on the basis of kinetic results and physical-chemical characterization measurements of the catalyst.

In the same year, Liu *et al.* has been studied the interaction between Mo species and HZSM-5 of Mo/HZSM-5 catalysts by using a high-resolution solid state nuclear magnetic resonance spectrometer with  $^{27}\text{Al}$  and  $^{29}\text{Si}$  probes. The results showed that there was a strong interaction between Mo species and HZSM-5 zeolite. The framework aluminum in the zeolite could be easily extracted by the introduction of Mo species. With increasing Mo loading and calcinations temperatures, the interaction develops so strong that all the aluminum in the framework can be extracted by Mo species, and at last forms a new  $\text{Al}_2(\text{MoO}_4)_3$  crystalline phase. The framework of ZSM-5 zeolite collapses at the end, and the catalytic activity for methane dehydrogenation and aromatization drops dramatically. The dealumination of the catalyst having a Mo loading of 15% and had been calcined at 973 K was severe that all the aluminum in the framework were extracted and no framework Al could be detected by  $^{27}\text{Al}$ -MAS-NMR. The catalyst lost its catalytic activity for methane dehydrogenation and aromatization in the absence of oxygen. The Si/Al ratio measured from  $^{29}\text{Si}$ -MAS-NMR further confirms the dealumination process observed by  $^{27}\text{Al}$ -MAS-NMR. The MAS-NMR results gave that  $\text{Al}_2(\text{MoO}_4)_3$  crystallites were much less active for the reaction.

In 1998, Weckhuysen *et al.* used X-ray photoelectron spectroscopy (XPS) to determine the state of the transition metal ions (V, Cr, Fe, W, and Mo) on impregnated and ion-exchanged HZSM-5 zeolites that were active for the catalytic conversion of methane to benzene at 750°C. During an induction period, transition metal suboxides were formed on all of the impregnated catalysts except Mo/HZSM-5 for which  $\text{Mo}_2\text{C}$  was formed. It appeared that the active phases were  $\text{Fe}_3\text{O}_4$ ,  $\text{V}_2\text{O}_3$ ,  $\text{Cr}_2\text{O}_3$ , and  $\text{WO}_2$  located on the external surface of the zeolite. Ion-exchanged samples became more active after treatment with CO at 500°C. For the Fe/HZSM-5 sample, this treatment resulted in the migration of the metal to the external surface of the zeolite and the formation of an iron oxide phase.

Zhang *et al.* (1998) also described the characterization of Mo/HZSM-5 zeolite catalysts active for the non-oxidative conversion of methane to benzene. FTIR,  $^{27}\text{Al}$  and  $^{29}\text{Si}$  NMR evidence was presented for migration of molybdenum into the zeolite pores during catalyst calcinations at high temperatures. Mo K-edge Extended X-ray Absorption Fine Structure (EXAFS) confirmed that calcinations produced highly dispersed oxomolybdenum or molybdate species which were converted to a molybdenum carbide phase under reaction conditions.

Liu *et al.* (1999) studied the acid sites and the interaction between Mo species and HZSM-5 of the different Mo loading on HZSM-5 by in situ FTIR spectroscopy using pyridine as the probe molecule. The relative adsorbed amount of pyridine bonded on Brønsted and Lewis acid sites was measured by using the relative integrated intensities of the pyridine bands at 1450 and 1540  $\text{cm}^{-1}$ . A band at 1450  $\text{cm}^{-1}$  was assigned to the vibration mode of pyridine adsorbed on Lewis acid sites or pyridine coordinately bonded to cations. A band at 1540  $\text{cm}^{-1}$  was pyridinium ions formed at Brønsted acid sites. Therefore, the ratio of intensities of the bands at 1540 and 1450  $\text{cm}^{-1}$  as a measure of the amount of pyridine adsorbed on Brønsted and Lewis acid sites. The intensity of the bands at 3618 and 3740  $\text{cm}^{-1}$  characteristic of surface OH groups appeared at 573 K. It appeared that Mo species dispersed and migrated into the channel and located on the hydroxyl groups associated with framework Al. The relative intensities of the bands at 3618 and 3740  $\text{cm}^{-1}$  decreased in the same way in Mo/HZSM-5 with a Mo loading lower than 3%, showing that Mo species locate either on the external surface or in an internal channel after calcinations at 773 K. Mo species preferably located on Lewis acid sites to a certain extent and then located on Brønsted acid sites. However at high Mo loading samples, Mo species preferably located on Brønsted acid sites. The pyridine molecules adsorption on Brønsted acid sites was much stronger than adsorbed on Lewis acid sites. The increasing in the intensity of the band at 1549  $\text{cm}^{-1}$  implies that new Lewis and Brønsted acid sites were generated on high Mo loading samples.

Ma *et al.* (2000) described Electron Paramagnetic Resonance (EPR) characterization of the Mo species on the HZSM-5 zeolite. Four different Mo species

form EPR signals were identified on the basis of their reducibility and the nature of the signal concerned. There were two kinds of Mo species on the Mo/HZSM-5 samples, which were located at different positions in the HZSM-5 zeolite. The first kind of the Mo species was polynuclear and located on the external surface. They were either in the octahedral-coordinated  $\text{MoO}_3$  crystallite form or in the  $\text{MoO}_x$  form with a square-pyramidal coordination. The second kind of the Mo species was associated with the Al atom in the lattice channels of the zeolite. The Mo species associated with Al are mononuclear species, which migrated or diffused into the channels of the HZSM-5 during calcinations. The EPR signals of migrating Mo ion had hyperfine structures caused by the interaction between the Mo species and the lattice Al atom. And the corresponding Mo species were located at two different positions close to the Brønsted Al atoms. The variation of the different Mo species in a 6%Mo/HZSM-5 sample during the reaction course was illustrated, and the relationship between the catalytic performance and the intensity of the Electron Spin Resonance (ESR) spectra was discussed. It was proposed that  $\text{Mo}_2\text{C}$  was located at the external surface, while partial reduced Mo species associated with the Al atom was inside the channel during the reaction. Both of these Mo species play a key role in methane dehydroaromatization.

In 2001, Chen *et al.* investigated the different contents of Mo were loaded on HZSM-5 and used for the methane conversion under nonoxidative conditions. XPS and in situ oxygen  $^{16}\text{O}_2$  and  $^{18}\text{O}_2$  adsorption FTIR analysis were carried out on the working catalysts that reacted with methane at initial stages for various times. The usage of oxygen in the pretreatment reduced the induction period of the reaction. The oxygen adsorbed at Al sites of catalysts during the treatment time and form  $\text{O}^{2-}$  species were studied by FTIR measurement. From XPS measurement revealed that some  $\text{Mo}^{6+}$  was reduced to  $\text{Mo}^{2+}$  in the form of carbide during the initial stage of the reaction. Increasing of Mo loading increased the ratio of  $\text{Mo}_2\text{C}$  to  $\text{MoO}_3$  on the surface, but maximized the benzene yield at 3wt% Mo loading. The optimum  $\text{Mo}_2\text{C}/\text{MoO}_3$  ratio was about 0.38. Brønsted acid sites of HZSM-5,  $\text{MoO}_3$  and  $\text{Mo}_2\text{C}$  might be the active phase for methane aromatization.

Ding *et al.* (2001) studied the structure and density of Mo species in Mo/HZSM5 during catalytic CH<sub>4</sub> reactions using in-situ X-ray absorption spectroscopy (XAS), temperature-programmed oxidation after reaction, and the isotopic exchange of D<sub>2</sub> with zeolitic OH groups in HZSM5 before and after CH<sub>4</sub> reactions. These methods revealed that CH<sub>4</sub> reactions caused exchanged Mo<sub>2</sub>O<sub>5</sub><sup>2+</sup> dimers and reduced to form small MoC<sub>x</sub> clusters with the concurrent regeneration of the bridging OH groups that were initially replaced by Mo oxo dimers during exchange. The inactive Mo oxo species activate in contact with CH<sub>4</sub> to form the two sites required for the bifunctional conversion of CH<sub>4</sub> to aromatics: MoC<sub>x</sub> for C-H bond activation and initial C-C bond formation and the Brønsted acid sites for oligomerization and cyclization of C<sub>2</sub> hydrocarbons to form stable aromatics. The Brønsted acid sites formed during carburization and oligomerization of MoC<sub>x</sub> species ultimately become covered with hydrogen-deficient reaction intermediates or unreactive deposits. The highly dispersed nature of the MoC<sub>x</sub> clusters was confirmed by detailed simulations of the XAS radial structure function and by the low temperatures required for the complete oxidation of these MoC<sub>x</sub> species compared with bulk Mo<sub>2</sub>C. Initial CH<sub>4</sub> reactions with MoO<sub>x</sub> precursors were stoichiometric and led first to the removal of oxygen as CO, CO<sub>2</sub>, and H<sub>2</sub>O and to the introduction of carbidic carbons into the reduced structures. C-H bond activation reactions become catalytic by the coupling of this activation step with the removal of the resulting CH<sub>x</sub> species, CH<sub>2</sub> appeared to be the most abundant surface fragment present during form C<sub>2</sub> hydrocarbons, which desorbs to reform the MoC<sub>x</sub> sites required for C-H bond activation steps.

Ha *et al.* (2002) attempted to understanding on the nature of active sites operating during the aromatization of methane over Mo/HZSM-5 catalyst. The role of protons in the zeolite and a reaction mechanism were examined. The reaction temperature was carried out at 973–1073K and atmospheric pressure. The migration of Mo species was studied by IR spectroscopy. Zeolite plays an important role for increasing Mo dispersion. IR analysis in the OH stretching vibrations showed that H<sup>+</sup> ions in HZSM-5 were exchanged during the calcinations of Mo/HZSM-5, and completely removed after the induction period at 823 K. At high temperature in

oxygen, molybdenum species migrated in the zeolite framework and replace  $H^+$ . These species were converted into  $Mo_2C$  by reaction with methane, residual carbon deposit poisoning the residual zeolite protons. The proton acid sites were not prerequisite for aromatization of  $C_2H_2$  or  $C_2H_4$ . The conversion of acetylene to aromatics proceeded more easily than the ethylene over HZSM-5 catalyst. It was concluded that the principal route for the aromatization of  $CH_4$  was the formation of  $C_2H_2$  as the primary product which was oligomerized over  $Mo_2C$  into polyene such as hexadiene and cyclized into aromatics.

Miao *et al.* (2004) investigated the characterization Mo/HMCM-22 catalysts with Inductively Coupled Plasma-Atomic Emission Spectrometry (ICP-AES), X-ray Diffraction (XRD),  $NH_3$  Temperature Programmed Desorption ( $NH_3$ -TPD) technique, Ultra Violet-Visible (UV-Vis) and UV Raman spectroscopy, the reactivity of Mo species for methane partial oxidation into formaldehyde were directly studied with a new point of view. By comparing the fresh and used catalysts, it was found that the tetrahedral Mo species bonding chemically to the support surface were practically unchanged after the reaction, while the polymolybdate octahedral Mo species, which had a rather weak interaction with the MCM-22 zeolite, leached out during the reaction, especially when the Mo loading was high. It was found from the time-on-stream reaction data that the HCHO yield remained unchanged, while  $CO_x$  decreased with the reaction time during the reaction. By combining the characterization results and the reaction data, it could be shown that the isolated tetrahedral molybdenum oxo-species was responsible for HCHO formation, while the octahedral polyoxomolybdate species led to the total oxidation of methane.

#### **4. The nature of the carbonaceous deposits and its role in the reaction**

The heavy carbon deposits formed during the methane dehydroaromatization is a major obstacle for understanding of the reaction and process development. Reduce the formation of the carbonaceous deposits in the methane dehydroaromatization is the great challenge for the potential industrial applications.

In 2001, Liu *et al.* studied of the carbon deposits formed on Mo/HZSM-5 catalyst in methane dehydroaromatization by using Thermalgravimetric analysis (TG) and temperature programmed techniques. From the H<sub>2</sub>-temperature programmed (TPH) experiment, there were active carbon-containing species on the coked Mo/HZSM-5 catalyst, which corresponding to benzene and ethylene were much larger than peak area of ethane. The peak temperature of benzene in the CO<sub>2</sub>-temperature programmed (TPCO<sub>2</sub>) higher than TPH experiment, probably some of the polyaromatics decomposed on the coke sample. The subsequent treatments of TPCO<sub>2</sub> and TPH were effective for reducing the amount of coke.

In 2003, Tan *et al.* investigated the nature of coke formed during methane aromatization by temperature programmed oxidation. The effects of adding O<sub>2</sub> and CO<sub>2</sub> to the methane are also discussed. The effects of H<sub>2</sub> and CO on the deactivation of the Mo/HZSM-5 catalyst were studied by temperature programmed surface and XPS studied. The results showed that the stability of the catalyst increased with oxygen concentration until 3.2vol% was reached. The increasing in the CO<sub>2</sub> concentration results decreased hydrocarbon and initial aromatic yields. The addition of hydrogen in the feed depressed methane conversion, increased the selectivity to C<sub>2</sub> hydrocarbon and C<sub>2</sub>H<sub>4</sub>/C<sub>2</sub>H<sub>6</sub> ratio, but decreased aromatic yields. The TPO results showed that there were two kind of carbon that was responsible for catalytic deactivation on the catalyst at 600°C. Three zones of different color were observed in the catalyst bed used for the aromatization of methane in the presence of oxygen. From the XPS spectra of Mo for the catalysts at the different zone, in a white zone was mainly in the form Mo<sup>6+</sup>. For the gray zone the appearance of peaks led to the overlap of Mo 3d doublets from Mo<sup>4+</sup>, Mo<sup>5+</sup>, Mo<sup>6+</sup>. In the black zone attribute to presence of the active Mo<sub>2</sub>C species. The XPS results indicated that partially reduced MoO<sub>3</sub>, i.e. MoO<sub>x</sub>C<sub>y</sub> into Mo<sub>2</sub>C species.

Ma *et al.* (2003) reported the effect of a small amount of hydrogen co-fed with methane for inhibition of the coke formation and stabilization of the catalytic activity of methane dehydroaromatization on Mo/HZSM-5 catalyst. Although the highest catalytic activities decreased with increasing H<sub>2</sub> partial pressure because of



thermodynamic limitation, the formation rate of aromatic products such as benzene, naphthalene and toluene were stabilized by the addition of hydrogen into feed gas. The coke formation especially on Brønsted acid sites were also suppressed during the methane dehydroaromatization reaction.

Su *et al.* (2003) used the NH<sub>4</sub>ZSM-5 zeolite treated with a NaOH solution of desirable concentration and followed exchanging with NH<sub>4</sub>OH solution for enhancing the activity and stability of Mo/HZSM-5 catalyst in methane dehydroaromatization process. Many small crystallites disappeared on the surface of catalyst after an alkaline treatment and large crystallites were dissolved and cracked by the alkaline treatment. From Scanning Electron Microscopy (SEM) images, it is clear that the mesopore has been created. The alkali treatment has no effect to the acidity in term of free Brønsted acid sites and the strength of the Brønsted acid sites. A proper alkali treatment could create amount of mesopores, which coexisted with the inherent micropores of the HZSM-5 zeolite due to the dissolution of siliceous species of the zeolite framework. The alkali treated Mo/HZSM-5 showed a very high catalytic performance and high tolerance to the carbon deposits in the conversion of methane to aromatics.

In the same year, Liu *et al.* studied the addition of a few percent of water to methane feed significantly improved catalytic performance in the methane dehydroaromatization reaction on 6 wt% Mo/HZSM-5 catalysts at 998–1073 K. The reforming reaction was accompanied with the dehydrocondensation reaction of methane. However, addition of water above 2.6% reduced the catalytic activity after several hours of time on stream. Coke was produced a lesser amount with increasing water concentration in methane feed. The HZSM-5 structure of Mo/HZSM-5 examined by XRD and <sup>27</sup>Al-MAS-NMR techniques remained intact even after the reaction at 1073 K in the presence of water except for a high water concentration of 2.6%, where framework aluminum migrated to extraframework positions, which decreased the catalytic activity. Small Mo<sub>2</sub>C clusters as an active species of the reaction were always observed on used catalysts by EXAFS analysis. Stabilities of Mo<sub>2</sub>C and carbon in a water atmosphere were discussed in conjunction with the

reactivity of coke formed on the catalyst during the methane dehydroaromatization reaction. Based on the above results, the reduction of catalytic activity at an excess addition of water may be explained by the two consecutive reactions. These two consecutive reactions proceed whenever coke was present on the catalyst but not on the catalyst having no coke. Therefore, water passed through on the catalyst having no coke and eventually almost all aluminum atoms in the lattice position move out by the action of water. Then, the catalyst could not promote the reforming reaction and also the dehydrocondensation reaction of methane.

In 2004, Ma *et al.* found that the Mo/HZSM-5 catalyst for methane aromatization at 1023 K removed the entire deposited hydrocarbon at 823 K by using pure air. Addition of a small amount of NO to air increased the coke removing ability. The deposited hydrocarbon on catalyst started to be removed above 603 K, and total coke removed at 723 K. Much lower regeneration temperature preventing any structure change of the Mo active sites suppressed the migration and sublimation of Mo species during the regeneration, which resulted in the very stable methane dehydroaromatization performance on the regenerated Mo catalyst. The formation rates of benzene decreased after the eighth regeneration cycle with NO addition to air, while the benzene formation rates of the catalyst regenerated with pure air started to decrease only after the fourth regeneration cycle.

## MATERIALS AND METHODS

### Materials

#### 1. Major equipment

- 1.1 Vertical tube furnace
- 1.2 Quartz tube
- 1.3 Mass flow controller sets
- 1.4 Gas Chromatography (GC)
- 1.5 Mass Spectrometer (MS)
- 1.6 Fourier Transform Infrared Spectrometer (FTIR)
- 1.7 Accelerated Surface Area and Porosimetry Analyzer (ASAP 2020)
- 1.8 X-ray Fluorescence Spectrometer (XRF)
- 1.9 Inductively Coupled Plasma-Atomic Emission Spectrometry (ICP-AES)

#### 2. Chemicals

- 2.1 ZSM-5 powder
- 2.2 Ammonium heptamolybdate ( $(\text{NH}_4)_6\text{Mo}_7\text{O}_{24} \cdot 4\text{H}_2\text{O}$ )
- 2.3 Iron (III) nitrate nonahydrate ( $\text{Fe}(\text{NO}_3)_3 \cdot 9\text{H}_2\text{O}$ )
- 2.4 Ammonium metavanadate ( $\text{NH}_4\text{VO}_3$ )
- 2.5 Ammonium nitrate ( $\text{NH}_4\text{NO}_3$ )
- 2.6 Hydrochloric acid (HCl)
- 2.7 Methane ( $\text{CH}_4$ )
- 2.8 Nitrous oxide gas ( $\text{N}_2\text{O}$ )
- 2.9 Oxygen gas ( $\text{O}_2$ )
- 2.10 Helium gas (He)
- 2.11 Hydrogen gas ( $\text{H}_2$ )
- 2.12 Nitrogen gas ( $\text{N}_2$ )
- 2.13 Argon gas (Ar)
- 2.14 Carbon monoxide (CO)

- 2.15 Carbon dioxide (CO<sub>2</sub>)
- 2.16 H<sub>2</sub> balanced Ar 2%
- 2.17 50% CH<sub>4</sub> balanced Ar
- 2.18 Benzene (C<sub>6</sub>H<sub>6</sub>)
- 2.19 Toluene (C<sub>7</sub>H<sub>8</sub>)
- 2.20 Liquid nitrogen (Liq. N<sub>2</sub>)

## **Experimental Methods**

### **1. Preparation of Catalysts**

#### **1.1 Preparation of HZSM-5 zeolites**

HZSM-5 zeolites with nominal SiO<sub>2</sub>/Al<sub>2</sub>O<sub>3</sub> ratios of 27 and 55 (ALSI-PENTA Inc.) were used as supports. 0.1 M of ammonium nitrate was used to exchange the remaining sodium cations at 80 °C for 24 hours, 3 times. This was followed by calcination at 550 °C for 5 hours in air to transform to acidic zeolites. These catalysts will be referred to (HZSM-5) SH27 and SH55, respectively.

#### **1.2 Preparation of transition metal ion exchanged HZSM-5**

The supported transition metals catalysts were prepared by ion exchanged with the aqueous solution of Fe(NO<sub>3</sub>)<sub>3</sub>·9H<sub>2</sub>O, NH<sub>4</sub>VO<sub>3</sub> and (NH<sub>4</sub>)<sub>6</sub>Mo<sub>7</sub>O<sub>24</sub>·4H<sub>2</sub>O at 80°C. The pH of iron aqueous solution was adjusted to the pH=1 by adding hydrochloric to prevent the precipitation of iron hydroxides. The slurry was made of 5 g of HZSM-5 and 250 ml of 0.1 M transition metal aqueous solutions and was continuously stirred for 6 h at 80 °C. Exchanged sample was filtered using filter paper (Whatman Laboratory No.42) and washed with deionization water (DI). Then, the samples were dried in oven at 80 °C overnight. The zeolites were calcined in air at 550 °C for 5 hours. Finally, the catalysts were pelleted, crushed and, then, sieved into 40-60 mesh size (0.250-0.425 mm).

### 1.3 Preparation of transition metal impregnated HZSM-5

The HZSM-5 zeolite samples about 5 g were added to aliquot amount of transition metal aqueous solution of  $\text{Fe}(\text{NO}_3)_3 \cdot 9\text{H}_2\text{O}$ ,  $\text{NH}_4\text{VO}_3$  and  $(\text{NH}_4)_6\text{Mo}_7\text{O}_{24} \cdot 4\text{H}_2\text{O}$  250 ml and the slurries were dried at 80 °C in a rotary evaporator. The samples were dried overnight at 80 °C in an oven. The resulting catalysts were calcined in air at 550 °C for 5 hours and sieved to 40-60 mesh size.

## 2. Characterization of catalysts

### 2.1 Elemental analysis

Elemental analysis of TM/SH27 and TM/SH55 samples were determined by XRF spectroscopy using Bruker AG XRS 3400 spectrometer and Inductively Coupled Plasma-Atomic Emission Spectrometry (ICP-AES) using Perkin Elmer model PLASMA-1000 for transition metals analysis.

### 2.2 Surface areas measurement

Nitrogen adsorption at liquid nitrogen temperature was performed to examine the pore volume of zeolite samples. The experiment was performed on a Micromeritics ASAP 2020 instrument. Prior to each measurement, 0.1 g of sample was degassed for 20 hours at 350 °C under vacuum. The specific surface area was calculated by Brunauer, Emmett, and Teller (BET) equation, while the micropore volume ( $V_{\text{micro}}$ ) was determined using the  $t$ -plot method with the Harkin-Jura equation between  $P/P_0$  values from about 0.05 to 0.3.

### 2.3 Fourier Transform Infrared Spectrometer (FTIR)

FTIR spectra of the samples were recorded in Diffuse Reflectance Infrared Fourier Transform (DRIFT) technique for observe the Brønsted acid sites in the range of 3,400-3,900  $\text{cm}^{-1}$ . The FTIR spectra were recorded with a Bruker IFS

66v/S FTIR spectrometer using  $\text{CaF}_2$  window and MCT detector. Samples were loaded in the DRIFT sample cup and placed into an infrared cell. To remove water adsorbed, the sample had heated (heating rate  $3\text{ }^\circ\text{C min}^{-1}$ ) in vacuum for  $400\text{ }^\circ\text{C}$  for 1.5 h and then cooled to  $30\text{ }^\circ\text{C}$  prior to obtaining the spectrum. Each spectrum was obtained from 32 scans taken at a resolution of  $2.0\text{ cm}^{-1}$ .

## **2.4 Temperature Programmed Reduction (TPR)**

Temperature programmed reduction (TPR) was performed to characterize the supported transition metals. The amount of catalyst ( $0.100\text{ g}$ ) was pretreated by  $10\%\text{O}_2/\text{Ar}$  (total flow  $60\text{ ml min}^{-1}$ ) heating in at  $550^\circ\text{C}$  for 2 h then cooled to room temperature in an argon flow before starting the reaction. The temperature program started at  $100\text{ }^\circ\text{C}$  with a heating rate of  $10\text{ }^\circ\text{C/min}$  under flow of hydrogen 2% in argon at a total flow rate of  $30\text{ ml/min}$ . The  $\text{H}_2$  consumption was detected by a Quadrupole Mass spectrometer (Quadstar QMS422).

## **3. Catalytic activity testing**

### **3.1 Flow reaction**

A fixed bed tubular reactor was used for catalytic activity testing. The quartz tube,  $60\text{ cm}$  long and  $0.43\text{ cm}$  i.d., was packed with quartz wool to hold  $0.050\text{ g}$  of the catalyst in place and covered with a layer of quartz beads to obtain a uniform gas distribution. The catalyst was pretreated under a  $10\%\text{O}_2/\text{He}$  ( $60\text{ ml/min}$ ) at  $600\text{ }^\circ\text{C}$  for 1 h, and then a  $10\%\text{H}_2/\text{He}$  ( $60\text{ ml/min}$ ) at  $550\text{ }^\circ\text{C}$  for 1 h. For steam treatment experiment, the sample was treated with a flow of  $\text{H}_2\text{O}/\text{N}_2$  ( $30\text{ ml/min}$  with a  $\text{H}_2\text{O}$  partial pressure of  $42.46\text{ mbar}$ ) at  $650\text{ }^\circ\text{C}$  for 2 h before the treatment with oxygen and hydrogen. The reaction gas was a mixture of  $2\%\text{H}_2$ ,  $10\%\text{CH}_4$ ,  $10\%\text{N}_2\text{O}$  and  $10\%\text{Ar}$  (as internal standard) and balance with He. The reaction conditions using in the experiment were as follows: reaction temperature,  $500\text{ }^\circ\text{C}$ ; total flow rate,  $100\text{ ml/min}$ ; pressure,  $1\text{ atm}$ ; time on stream,  $15\text{ min}$ . The products were analyzed by on-line gas chromatography (Trace GC) with a column packing is Porapak Q and

Hayesep D for the separation of gas products and a thermal conductivity (TCD) detector and Quadrupole Mass spectrometer (Quardstar QMS422). The mass fragments were measured at  $m/e = 2, 15, 18, 28, 30, 40, 44, 78$ , and 91 for  $H_2$ ,  $CH_4$ ,  $H_2O$ ,  $CO$ ,  $N_2O$ ,  $Ar$ ,  $CO_2$ ,  $C_6H_6$ , and  $C_7H_8$ , respectively.

A schematic diagram of the experimental setup is shown in figure 1.

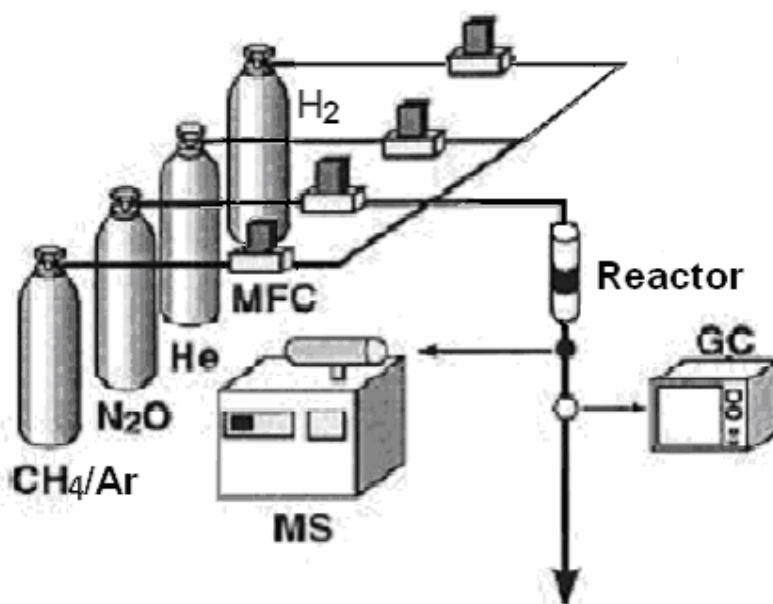


**Figure 1** Experimental setup

### 3.2 Pulse Reaction

Measurements were performed on the same equipment and used the same pretreatment conditions as the flow reaction. The reaction gas was a mixture of  $CH_4$ ,  $N_2O$ , and  $H_2$ . Helium flow rate 50 ml/min used as the carrier gas. The reaction condition using in the experiment were as follows: reaction temperature, 500 °C; pressure, 1 atm; pulse volume 1 ml, 60 pulses.

#### 4. Calculation Methods

Conversion and selectivity were calculated based on total converted atomic carbon.

$$\text{methane conversion} = \frac{[CH_4]_{(inlet)} - [CH_4]_{(outlet)}}{[CH_4]_{(inlet)}} \times 100\%$$

*selectivity to benzene and toluene*

$$= \frac{\text{moles of atomic carbon in benzene or toluene}}{\text{moles of converted atomic carbons}} \times 100\%$$

$$\text{yield} = \frac{(\text{conversion}) \times (\text{selectivity})}{100} \%$$

$$\text{Formation rate} = \frac{PF_t \text{ mol}_{B/T}}{RTW_c}$$

$$\begin{aligned} \text{Carbon balance} &= \frac{\text{moles of atomic carbon in gaseous products}}{\text{total converted atomic carbon}} \times 100\% \\ &= \frac{[7 \times \text{mol}T + 6 \times \text{mol}B + \text{mol}CO + \text{mol}CO_2]_{(outlet)}}{\text{mol}[CH_4]_{(inlet)} - CH_4]_{(outlet)}} \times 100\% \\ &= 100 \pm 10\% \end{aligned}$$

$$\begin{aligned} \text{Oxygen balance} &= \frac{\text{moles of atomic oxygen in gaseous products}}{\text{total converted nitrous oxide}} \times 100\% \\ &= \frac{[3 \times \text{mol}CO + 4 \times \text{mol}CO_2]_{(outlet)}}{\text{mol}[N_2O]_{(inlet)} - N_2O]_{(outlet)}} \times 100\% \\ &= 100 \pm 20\% \end{aligned}$$

Where; P represents to the pressure of gas,  $F_t$  denotes to total volumetric flow of feed gas, mol stands for moles of products, R means gas constant, T refers to temperature, and  $W_c$  indicates weight of catalyst. Carbon and oxygen balances were calculated to check the consistency of the concentration measurement.



## RESULTS AND DISCUSSION

### 1. Characterization of catalysts

#### 1.1 Elemental Analysis

The results of the elemental analysis of transition metals supported on HZSM-5 with the different of Si/Al ratio determined by X-ray Fluorescent spectrometry (XRF) and Inductively Coupled Plasma-Atomic Emission Spectrometry (ICP-AES) showed at Table 1.

**Table 1** Elemental analysis for all samples by XRF and ICP-AES techniques.

Sample	Molar ratios of the samples using XRF			TM (wt%) using ICP-AES
	Si/Al	TM/Al	TM (wt%)	
impFe/SH27	22.1	0.30	1.63	2.08
impV/SH27	21.9	0.32	1.94	1.57
impMo/SH27	22.4	0.07	0.34	0.27
Ex-Fe/SH27	23.4	0.02	0.10	0.08
Ex-V/SH27	21.8	-	*	0.01
Ex-Mo/SH27	21.5	-	*	0.02
Ex-Fe/SH55	40.2	0.02	0.06	0.04
Ex-V/SH55	39.9	-	*	0.004
impMo/SH55	39.2	0.14	0.41	0.25

\* not detectable by XRF

The transition metal contents for all samples determined by ICP-AES were somewhat smaller than using XRF method. The XRF measuring metal contents were 1.63, 1.94, 0.34 and 0.41% for impregnated Fe, V, and Mo on SH27 and Mo on SH55, respectively which were significantly smaller than the expected values of 2 %wt for all metals. The ion exchange samples contained very small amount of metal approximately 0.1 %wt for Fe and undetectable amount for V and Mo by XRF

method, though ICP-AES method detected a small amount of V and Mo, indicating the difficulties in exchange these metal ions with the zeolitic proton. The iron exchange was done in an acidic solution to prevent the formation of iron hydroxides but the acidic condition may also obstruct the exchange of the zeolite acid protons with the iron ions. As a result, only 2% of the Brønsted acids were exchanged. On the other hand, the  $V^{n+}$  and  $Mo^{n+}$  ions in solution may be present in the forms that were not suitable for the ion exchange with the zeolitic proton, for example, in the form of negative ion complex (Lucas *et al.* (2000) and Tan *et al.* (2002)) or having too high positive charge.

### 1.2 Specific Surface Areas and Porosity

**Table 2** BET Surface Areas and Micropore Volumes of the transition metals supported HZSM-5 catalysts

Samples	BET	<i>t</i> -Plot			
	$S_{BET}$ (m <sup>2</sup> /g)	$S_{ext}$ (m <sup>2</sup> /g)	$V_{total}$ (cm <sup>3</sup> /g)	$V_{micro}$ (cm <sup>3</sup> /g)	$V_{meso}^a$ (cm <sup>3</sup> /g)
SH27	396.0	32.27	0.191	0.149	0.042
impFe/SH27	385.7	45.83	0.194	0.140	0.055
impV/SH27	369.7	24.04	0.171	0.141	0.030
impMo/SH27	394.3	48.81	0.198	0.142	0.056
Ex-Fe/SH27	400.6	44.10	0.197	0.146	0.051
Ex-V/SH27	394.0	48.82	0.195	0.144	0.051
Ex-Mo/SH27	366.9	38.64	0.179	0.135	0.044
SH55	364.2	101.12	0.174	0.107	0.067
Ex-Fe/SH55	339.4	92.50	0.161	0.100	0.061
Ex-V/SH55	361.8	98.66	0.177	0.107	0.070
impMo/SH55	361.7	96.38	0.168	0.108	0.060

$$^aV_{mesopore} = V_{total} - V_{micropore}$$

BET surface areas and porosimetry analyses of the catalysts are shown in the Table 2. The introduction of transition metal led to a loss in surface areas and

micropore volumes of the zeolites. This is because that some metal ions or metal clusters may be present in the pore of the zeolite and partially block the channels of HZSM-5 zeolites and thus reduce the surface areas and the micropore volumes of the catalysts. The slight increase of the external surface of catalyst may be due to the aggregation of the metal oxide on outer surface. The SH27 and the TM/SH27 samples had higher surface areas and micropore volume than the SH55 and the TM/SH55 samples. However, the SH55 samples had higher external surface areas and mesopore volume. These two supports had different compositions. They contained  $\text{SiO}_2/\text{Al}_2\text{O}_3$  of 22 and 40 for SH27 and SH55, respectively.

### 1.3 FTIR studied

The structure and Brønsted acid sites characteristics of the samples were investigated by FTIR spectroscopy. The FTIR spectrum observed the Brønsted acid sites in the wavenumber regions of  $3,400\text{--}3,900\text{ cm}^{-1}$  as following with Fig. 2-4.

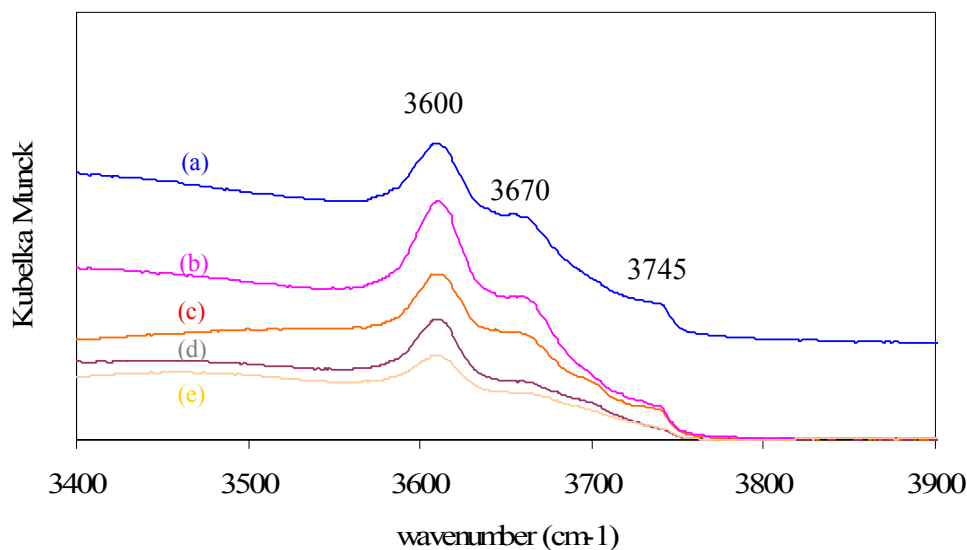


**Figure 2** Normalized FTIR spectra of the OH stretching region of HZSM-5 and Fe/HZSM-5 samples heated at  $400\text{ }^{\circ}\text{C}$  for 1.5 h: (a) SH27; (b) impFe/SH27; (c) Ex-Fe/SH27; (d) SH55; (e) Ex-Fe/SH55

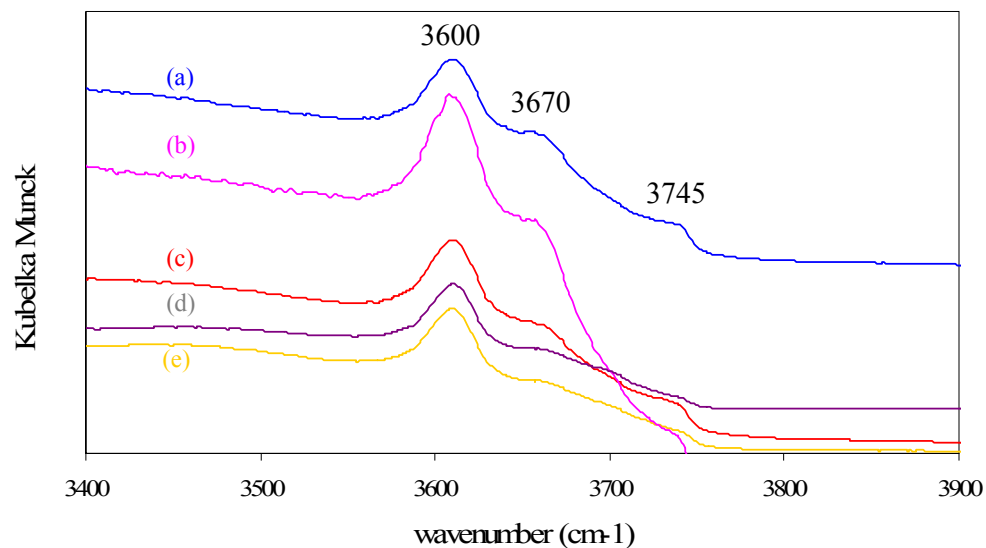


**Figure 3** Normalized FTIR spectra of the OH stretching region of HZSM-5 and V/HZSM-5 samples heated at 400 °C for 1.5 h: (a) SH27; (b) impV/SH27; (c) Ex-V/SH27; (d) SH55; (e) Ex-V/SH55

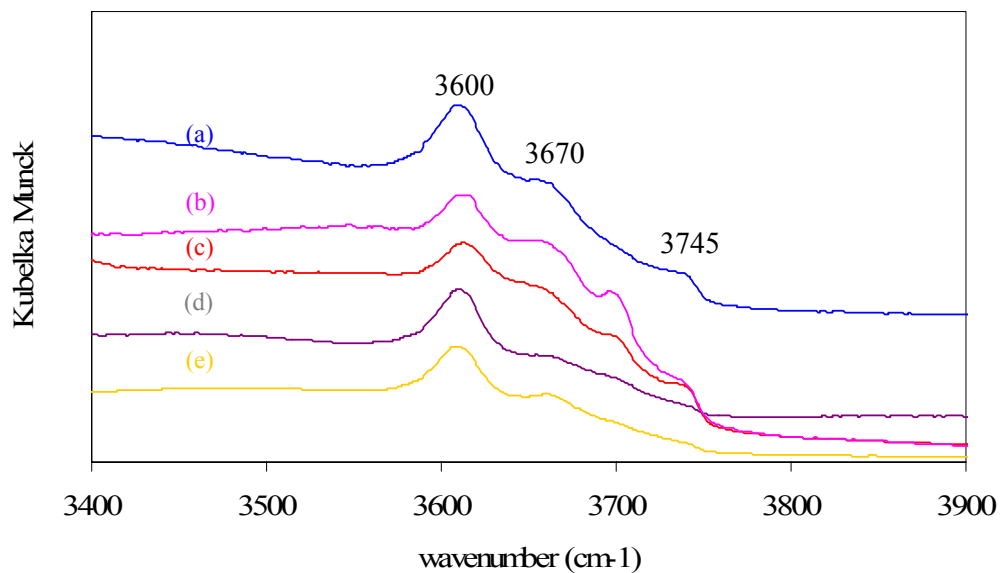


**Figure 4** Normalized FTIR spectra of the OH stretching region of HZSM-5 and Mo/HZSM-5 samples heated at 400 °C for 1.5 h: (a) SH27; (b) imp2%Mo/SH27; (c) Ex-Mo/SH27; (d) SH55; (e) impMo/SH55

**Table 3** Summarized FTIR spectra of modified and unmodified HZSM-5 zeolites

Wave number (cm <sup>-1</sup> )	Assignments	Reference
3610	OH stretch of Brønsted acid sites	1,3,4
3670	OH groups associated with extraframework Al species	1,3,4
3745	Silanol group (Si-OH)	1,2,4

Sources: (1) Peras *et al.* (1992); (2) Zhang *et al.* (1998); (3) Lobree *et al.* (1999); (4) Liu *et al.* (2001)

The summarized FTIR spectra of modified and unmodified HZSM-5 zeolites showed in Table 3. The infrared spectra for zeolites in the hydroxyl stretching region are shown in Fig. 2-4. The IR spectra were recorded at 30 °C after the thermal treatment at 400 °C under vacuum to remove the adsorbed water molecules. The results showed that a rather strong broad band at around 3,610 cm<sup>-1</sup>, corresponding to bridging Si(OH)Al groups is characteristic of strong Brønsted acid sites in zeolites. The intensity of this band depends on the amount of the acidic sites in the zeolite which depends on the Si/Al ratio. The SH27 sample with higher Al content, thus higher acidity showed stronger peak at 3,610 cm<sup>-1</sup>. This band was slightly reduced after the exchange with metal cations indicating that some of the Brønsted acid protons were replaced by the metal cations. Because of the low loading, most of the Brønsted acid protons were preserved in the samples. The vibration band around 3,745 cm<sup>-1</sup> corresponding to stretching vibrations of isolated silanol (Si-OH) groups was observed, This band was assigned to the terminal silanol groups located on the external surface which are weakly acidic. The IR band at 3,670 cm<sup>-1</sup> which is assigned to hydroxyl groups on extraframework aluminum species was also observed. These bands were very general and occurred in all samples.

#### 1.4 Temperature Programmed Reduction of Hydrogen ( $H_2$ -TPR)

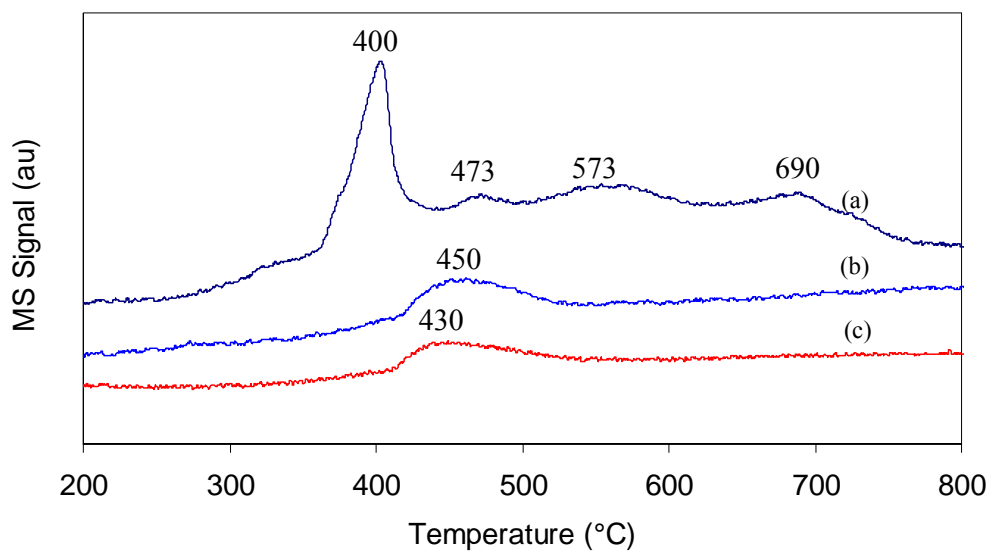


**Figure 5** Temperature programmed reduction profiles of Fe/HZSM-5 zeolites: (a) impFe/SH27; (b) Ex-Fe/SH27; (c) Ex-Fe/SH55.

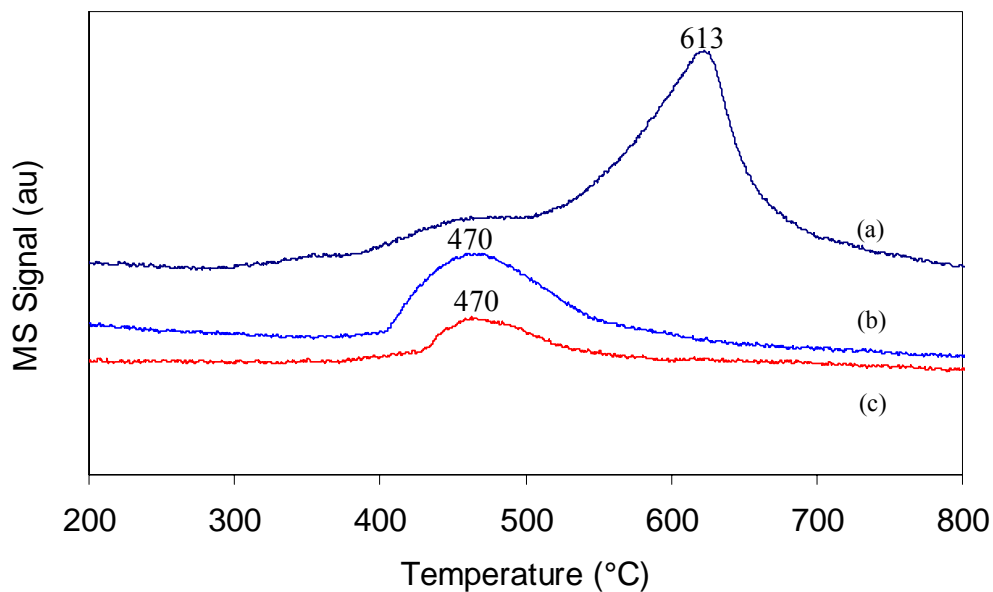


**Figure 6** Temperature programmed reduction profiles of V/HZSM-5 zeolites: (a) impV/SH27; (b) Ex-V/SH27; (c) Ex-V/SH55.

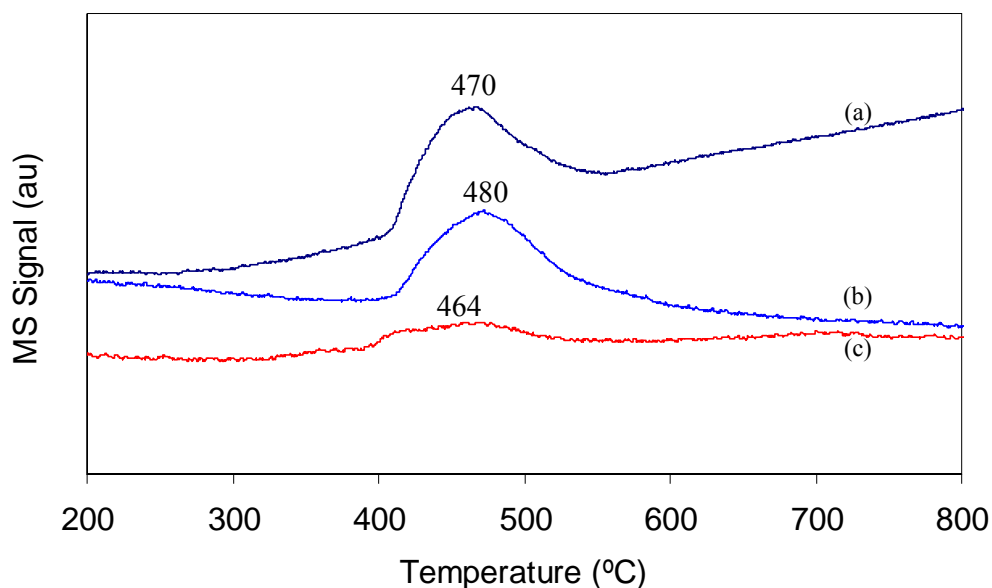


**Figure 7** Temperature programmed reduction profiles of Mo/HZSM-5 zeolites:  
(a) impMo/SH27; (b) Ex-Mo/SH27; (c) impMo/SH55.

The TPR profile of impregnated Fe/SH27 sample showed reduction peaks at 400 °C, 473 °C, 573 °C and 690 °C. The reduction peaks at 420 °C and 690 °C were corresponding to the reduction of bulk  $\text{Fe}_2\text{O}_3$  to  $\text{Fe}_3\text{O}_4$  and  $\text{Fe}_3\text{O}_4$  to  $\text{FeO}$ , respectively. The peak at 573 °C which was assigned to the reduction of exchanged  $\text{Fe}^{3+}$  to  $\text{Fe}^0$ . This TPR peak was also observed by Lobree *et al.* (1999). The Fe species of Ex-Fe/SH27 and Ex-Fe/SH55 were reduced at 450 °C and 430 °C from  $\text{Fe}^{3+}$  to  $\text{Fe}^{2+}$  of very small iron oxide clusters. This result was quite strange. However, it was similar to the TPR of  $\text{Fe/SiO}_2$  where the iron oxide formed small clusters such that they were stable against reduction to metallic iron during  $\text{H}_2$  reduction (Lobree *et al.* (1999)).

Weckhuysen *et al.* (2003) reported that vanadium oxide catalysts can be prepared by impregnation with an aqueous solution of  $\text{NH}_4\text{VO}_3$  or  $\text{NH}_4\text{VO}_3$  dissolved in aqueous oxalic acid. After calcination in air, vanadium oxides were oxidized mainly to the +5 oxidation state, vanadium pentoxide ( $\text{V}_2\text{O}_5$ ). The TPR peak at 613 °C corresponding to the reduction of  $\text{V}_2\text{O}_5$  to  $\text{V}_2\text{O}_3$  was observed for the  $\text{H}_2$

reduction of impV/SH27. While the TPR profile of vanadium exchanged samples showed a reduction peak at much lower temperature ( $\sim 470^\circ\text{C}$ ) indicated the exchanged vanadium species were clearly in the different states. This TPR peak may come from the reduction of  $[\text{VO}]^{2+}$  to  $\text{V}^{4+}$  as also observed by Dimitrova *et al.* (2004) or from the reduction of iron impurity that also occurred at around  $470^\circ\text{C}$ .

$\text{Mo}_7\text{O}_{24}^{6-} (\text{O}_h)$  was predominating in impregnated solution (Lucas *et al.* (2000) and Tan *et al.* (2002)) and the main species of molybdenum was isolated heptamolybdate ions in the uncalcined Mo/HZSM-5 catalyst (Chen *et al.* (1995)). During the impregnation and calcinations some molybdenum species were dispersed in the channels of the zeolite and interact with the Brønsted sites forming tetrahedral Mo species, which led to the change in the chemical environment of molybdenum atom, and the large size of Mo species were located on the external surface of the support blocking its channels in some extent. Tan *et al.* (2002) reported the  $\text{H}_2$  reduction profile of Mo/HZSM-5 that the reduction of Mo(VI) to Mo(V) of tetrahedral coordinated Mo species occurred at  $470^\circ\text{C}$  and the complete reduction of Mo(V) to Mo(IV) of octahedral coordinated Mo on poly- $\text{MoO}_3$  species which located on the outside of the HZSM-5 occurred at  $535^\circ\text{C}$ . In this work, the TPR of all Mo/HZSM-5 samples showed the reduction peak around  $470^\circ\text{C}$  which indicated that the Mo was in the form of tetrahedral coordinated  $\text{MoO}_3$ .

## **2. Catalytic Activity**

The reactions of partial oxidation of methane were performed in a microtubular reactor. The feeds were composed of  $\text{CH}_4$ ,  $\text{N}_2\text{O}$ ,  $\text{H}_2$ , Ar, and He and the reaction temperature was  $500^\circ\text{C}$ . The accurate determinations of the concentration of the complex product mixture were achieved using frequent calibrations of the mass fragmentation factor of individual compound compared with Ar as internal standard and deconvolution calculation for overlapping mass fragments of product mixture.



## 2.1 Catalytic performance of various catalysts at 500°C

**Table 4** Catalytic performance of various catalysts at 500 °C in the feed gas 10%CH<sub>4</sub>:

10%N<sub>2</sub>O: 2%H<sub>2</sub>:10%Ar and flow rate 100 ml/min

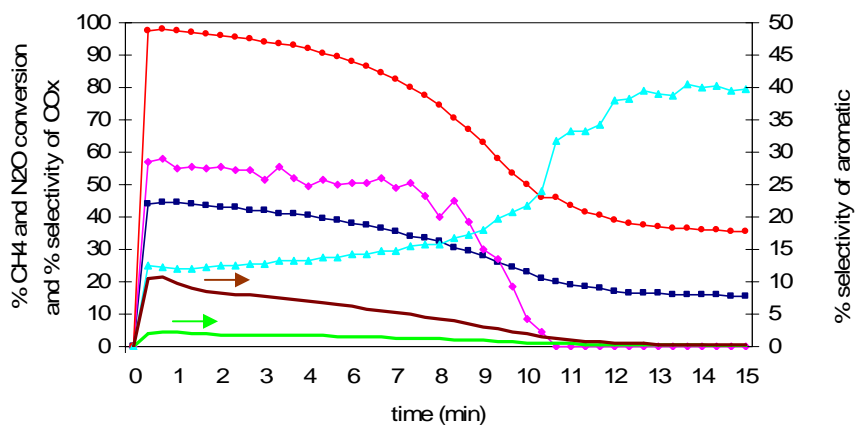
Samples	Conversion (mol%)		S <sub>Ar</sub> <sup>a</sup>	Y <sub>Ar</sub> <sup>a</sup>	Formation Rate <sup>a</sup> (μmol/s.gcat)		Deactivation time <sup>b</sup> (min)
	CH <sub>4</sub>	N <sub>2</sub> O			Benzene	Toluene	
SH27	61.7	95.6	7.52	4.03	0.92	4.97	4.94
impFe/SH27	34.4	99.3	0.46	0.16	0.06	0.16	1.80
Ex-Fe/SH27	42.8	96.7	10.1	4.32	0.84	4.13	5.82
impV/SH27	37.5	96.3	0.36	0.14	0.11	0.37	1.70
Ex-V/SH27	44.4	97.8	13.2	5.86	1.01	4.67	4.53
impMo/SH27	48.0	97.5	7.28	3.49	0.89	2.94	8.55
Ex-Mo/SH27	37.5	87.5	15.5	5.81	0.75	4.03	3.61

S<sub>Ar</sub>= Selectivity of aromatics (mol%)

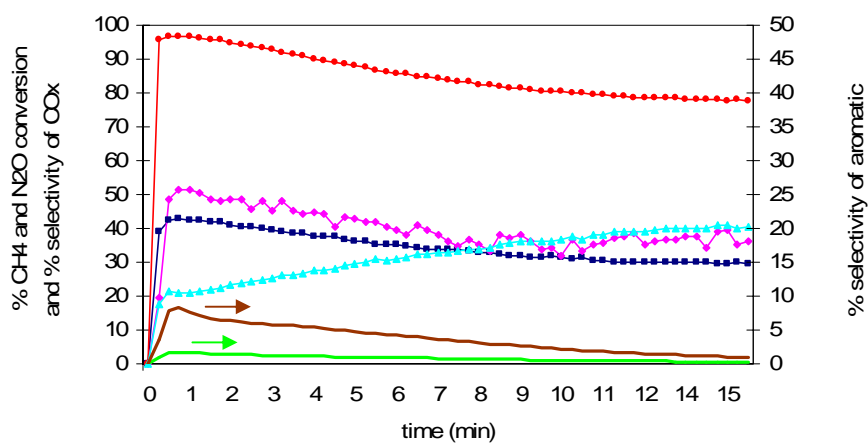
Y<sub>Ar</sub>= Yield of aromatics (mol%)

<sup>a</sup>data were recorded at maximum value

<sup>b</sup>deactivation time was time at a half of highest selectivity of aromatic

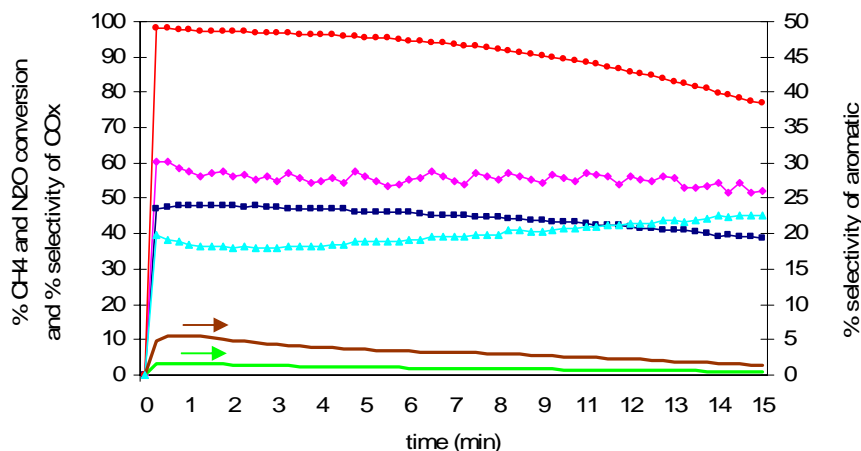


(a) Ex-V/SH27



(b) Ex-Fe/SH27

**Figure 8** The %conversion of methane and nitrous oxide and % selectivity of products of catalyst at 500 °C in the feed gas 10%CH<sub>4</sub>: 10%N<sub>2</sub>O: 2%H<sub>2</sub> and flow rate 100 ml/min: (a) Ex-V/SH27, (b) Ex-Fe/SH27, (c) impMo/SH27; %conversion of methane (■), nitrous oxide (●); %selectivity of carbon monoxide (◆), carbon dioxide (▲), benzene (—), and toluene (—).



(c) impMo/SH27

**Figure 8** (cont'd)

The results in Table 4 and Figure 8 showed that in the reaction carbon oxides were the major products with combined selectivity of ~90 %. The initial nitrous conversion was almost complete and slightly decreased with reaction time. The nitrous conversion was always higher than the methane conversion. The formation of benzene and toluene was also observed with combined selectivity up to 15 % carbon base. It was observed that selectivity for toluene was higher than that of benzene for all samples. This was different from the aromatic formation studied by other researchers such as Ding *et al.* (2001), where the benzene formation was higher than other aromatics. The HZSM-5 (SH27) sample had a low selectivity for aromatic (benzene and toluene). The metal exchanged samples showed improved aromatic selectivity. It was observed that no other small hydrocarbons (C2, C4) or higher aromatics observed in any significant amount.

The selectivity and the yield of aromatics of impregnated transition metal supported on HZSM-5 were even smaller than the selectivity of the starting zeolite because the metal oxide particles supported on zeolites may be present in the forms

that are more active for oxidation of methane to carbon oxides than the formation of aromatics products. Except for impMo/SH27 the selectivity for aromatics was comparable to that of the starting zeolite. In all case, the catalysts suffered severe coke deposition and lost their activity in minutes. Introduction of metals improved catalysts' life a little bit for Ex-Fe, Ex-V, and impMo on SH27 zeolites.

## 2.2 Effect of the ratio of CH<sub>4</sub> to N<sub>2</sub>O

**Table 5** Effect of the ratio of CH<sub>4</sub>/N<sub>2</sub>O on the catalytic performance in the presence of H<sub>2</sub> at 500 °C

Samples	CH <sub>4</sub> /N <sub>2</sub> O = 1			CH <sub>4</sub> /N <sub>2</sub> O = 2			CH <sub>4</sub> /N <sub>2</sub> O = 4		
	$\chi_{CH_4}$	$S^a_{Ar}$	$Y^a_{Ar}$	$\chi_{CH_4}$	$S^a_{Ar}$	$Y^a_{Ar}$	$\chi_{CH_4}$	$S^a_{Ar}$	$Y^a_{Ar}$
SH27	61.7	7.52	4.03	35.0	15.5	5.45	29.0	14.4	4.18
Ex-Fe/SH27	42.8	10.1	4.32	22.0	22.1	4.86	15.5	16.9	2.61
Ex-V/SH27	44.4	13.2	5.86	24.9	20.2	5.03	14.9	20.5	3.05
impMo/SH27	48.0	7.28	3.49	33.5	11.2	3.75	15.2	23.1	3.51

$\chi_{CH_4}$  = Conversion of methane (mol%)

$S_{Ar}$  = Selectivity of aromatics (mol%)

$Y_{Ar}$  = Yield of aromatic (mol%)

<sup>a</sup>data were recorded at maximum value

The ratio of CH<sub>4</sub>/N<sub>2</sub>O had effects on catalytic activities as shown in Table 5 and Figure 9. The nitrous oxide conversion was almost complete in all cases. Conversion of methane decreased when CH<sub>4</sub>/N<sub>2</sub>O ratio increased. On the other hand, the aromatic selectivity was increased with the CH<sub>4</sub>/N<sub>2</sub>O ratio. The maximum selectivity for aromatics was reached 20 % at CH<sub>4</sub>/N<sub>2</sub>O ratio of 2. Except for impMo/SH27, increased the CH<sub>4</sub>/N<sub>2</sub>O ratio to 4 did not result in the improved selectivity and yield for aromatics. Therefore, the CH<sub>4</sub>/N<sub>2</sub>O ratio of 2 seemed to be the optimized number.

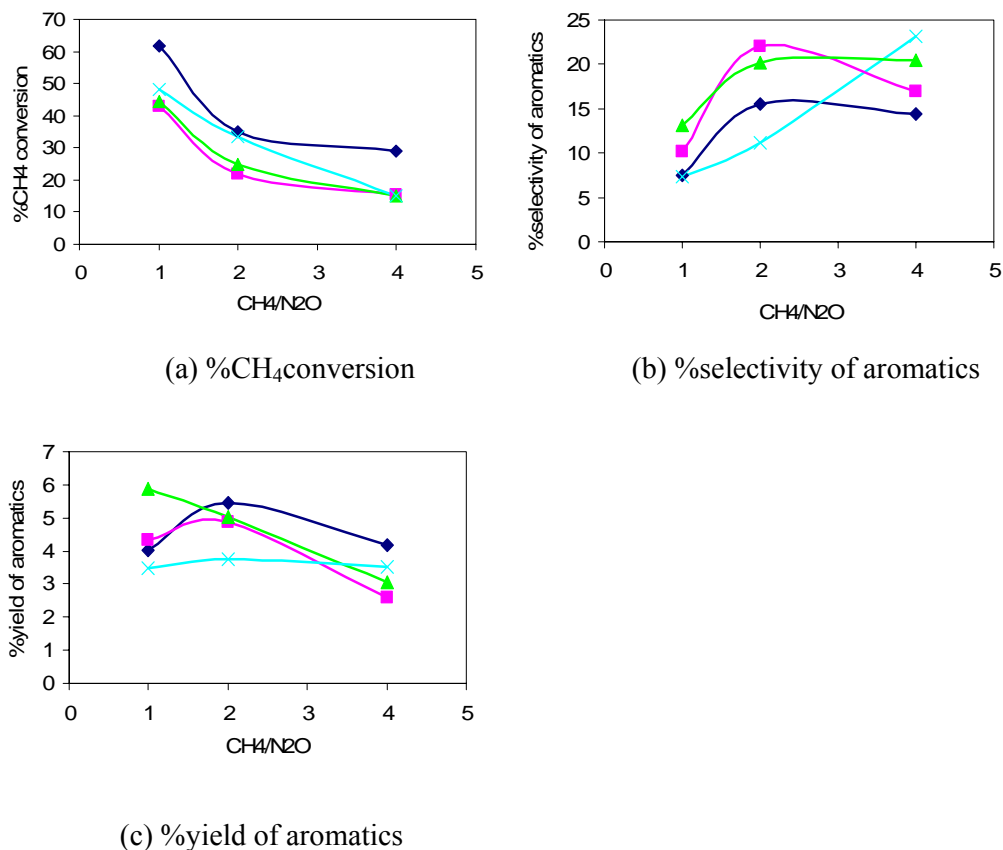


**Figure 9** Effect of the ratio of  $\text{CH}_4/\text{N}_2\text{O}$  on the catalytic performance in the presence of  $\text{H}_2$  at 500 °C: (a) %CH<sub>4</sub> conversion; (b) %selectivity of aromatics; (d) %yield of aromatics: ( $\blacklozenge$ ) SH27, ( $\blacksquare$ ) Ex-Fe/S, ( $\blacktriangle$ ) Ex-V/S, ( $\times$ ) impMo/S

### 2.3 Effect of Si/Al ratio

The effect of Si/Al ratio on catalytic activity is shown in Table 6 and Fig. 10. The selectivity of aromatic and the deactivation time decreased with increasing of Si/Al ratio. The rate of benzene and toluene formation on all catalysts decreased as the Si/Al increased with the same result of Ha *et al.* (2002). The acidity of zeolites decreased as Si/Al increased, because the high the Si/Al ratio lesser the number of exchangeable  $\text{H}^+$ . The increasing of Si/Al renders less probable the stabilization of atomically dispersed metal species.

**Table 6** Effect of Si/Al ratio on the catalytic performance of catalysts in methane aromatization in the feed 10%Ar:10%CH<sub>4</sub>:5%N<sub>2</sub>O:2%H<sub>2</sub> at 500 °C

Samples	Conversion				Formation Rate <sup>a</sup>		Deactivation time <sup>b</sup> (min)
	(mol%)		S <sub>Ar</sub> <sup>a</sup>	Y <sub>Ar</sub> <sup>a</sup>	(μmol/s.gcat)		
	CH <sub>4</sub>	N <sub>2</sub> O			Benzene	Toluene	
SH27	35.0	86.3	15.5	5.25	0.78	4.82	4.45
SH55	50.2	97.0	8.64	4.34	0.77	4.50	4.65
Ex-Fe/SH27	22.0	92.2	22.1	4.86	0.54	4.29	6.26
Ex-Fe/SH55	20.3	80.2	16.2	3.29	0.74	4.75	4.43
Ex-V/SH27	24.9	94.1	20.2	5.03	0.86	4.60	5.53
Ex-V/SH55	26.5	90.0	16.8	4.45	0.55	3.59	4.25
impMo/SH27	33.5	94.2	11.2	3.75	0.81	4.13	7.70
impMo/SH55	43.2	97.2	4.95	2.14	0.45	1.86	3.70

S<sub>Ar</sub> = Selectivity of aromatics (mol%)

Y<sub>Ar</sub> = Yield of aromatics (mol%)

<sup>a</sup>data were recorded at maximum value

<sup>b</sup>deactivation time was time at a half of highest selectivity of aromatic

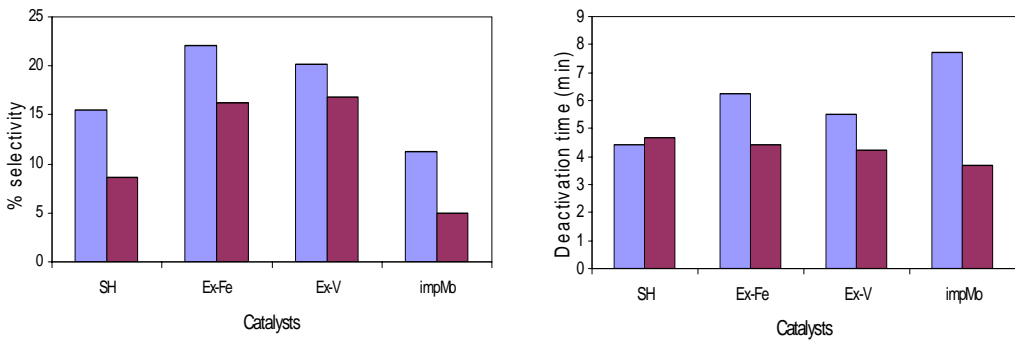
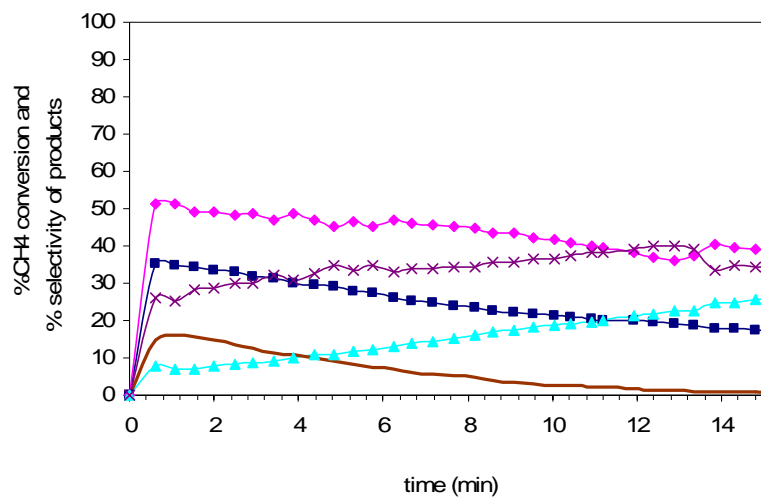
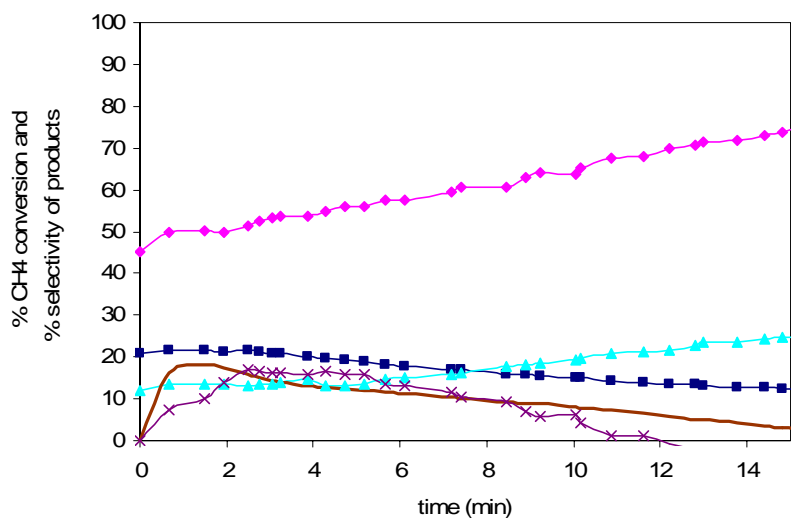


**Figure 10** Effect of Si/Al ratio on the catalytic performance of catalysts in methane aromatization in the feed 10%Ar:10%CH<sub>4</sub>:5%N<sub>2</sub>O:2%H<sub>2</sub> at 500 °C: (■) SH27 and (■) SH55



(a) SH27



(b) Ex-Fe/SH27

**Figure 11** The %conversion of methane and % selectivity of products of catalyst at 500 °C in the feed gas 10%CH<sub>4</sub>: 5%N<sub>2</sub>O: 2%H<sub>2</sub> and flow rate 100 ml/min: (a) SH27, (b) Ex-Fe/SH27; %conversion of methane (■); %selectivity of carbon monoxide (◆), carbon dioxide (▲), aromatic (—), and coke (x)

Form the results of Fig. 11 and Table 6 that compared the activity and stability of SH27 and Ex-Fe/SH27, we found that although the conversion of methane on SH27 was higher than Ex-Fe/SH27, the selectivity for aromatics was about half of that of Ex-Fe/SH27. Therefore, the yield of aromatic on these catalysts was about the same. However, the deactivation time of SH27 was shorter than Ex-Fe/SH27. It was estimated that as much as 30% of methane conversion on the SH27 resulted in coke formation. The exchange iron reduced the selectivity for coke formation to approximately ~15%.

#### 2.4 Effect of the steam treatment

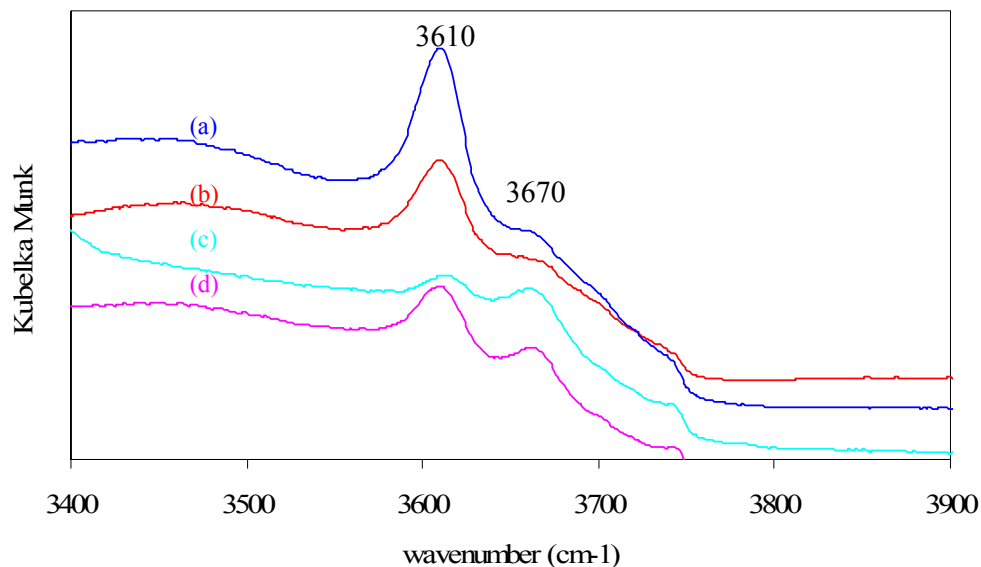


**Figure 12** Normalized FTIR spectra of the OH stretching region of samples heated at 400 °C for 1.5h: (a) Ex-V/SH55; (b) Ex-Fe/SH55; (c) steam Ex-V/SH55; (d) steam Ex-Fe/SH55.



**Table 7** BET Surface Areas and Micropore Volumes of steamed and unsteamed catalysts

Samples	BET	<i>t</i> -Plot			
	$S_{\text{BET}}$ ( $\text{m}^2/\text{g}$ )	$S_{\text{ext}}$ ( $\text{m}^2/\text{g}$ )	$V_{\text{total}}$ ( $\text{cm}^3/\text{g}$ )	$V_{\text{micro}}$ ( $\text{cm}^3/\text{g}$ )	$V_{\text{meso}}^{\text{a}}$ ( $\text{cm}^3/\text{g}$ )
Ex-Fe/SH27	400.6	44.10	0.197	0.146	0.051
Ex-V/SH27	394.0	48.82	0.195	0.144	0.051
Ex-Fe/SH27_ST	335.8	87.99	0.163	0.100	0.063
Ex-V/SH27_ST	323.0	80.45	0.159	0.098	0.061

ST = steamed sample

The effect of steam treatment on FTIR spectra of the OH stretching region and the surface and porosimetry analysis of steamed and unsteamed samples are shown in Fig. 12 and Table 7, respectively. After steam treatment at 650 °C, the band at 3610  $\text{cm}^{-1}$  was remarkably diminished indicating that the concentration of the Brønsted acid sites was significantly reduced, while the band at 3,670  $\text{cm}^{-1}$  emerged. This band is usually assigned to extraframework aluminum species. Steam treatment induced the extraction of tetrahedral Al to extraframework position and creating a more uniformed pore wall (Groen *et al.* (2003)). The Al extraction was followed by Si migration to stabilize the framework. From Table 7, the steam treatment caused the reduction of the surface areas and the micropore volumes from 400 to 330  $\text{m}^2/\text{g}$  and from 0.14 to 0.10  $\text{cm}^3/\text{g}$  but increased the mesopore volume and the external surface areas from 0.05 to 0.06  $\text{cm}^3/\text{g}$  and from 44 to 80  $\text{m}^2/\text{g}$ , respectively.

**Table 8** Effect of the steam treatment on methane aromatization in the feed  
10%Ar:10%CH<sub>4</sub>:5%N<sub>2</sub>O:2%H<sub>2</sub> at 500 °C with flow rate 100 ml/min

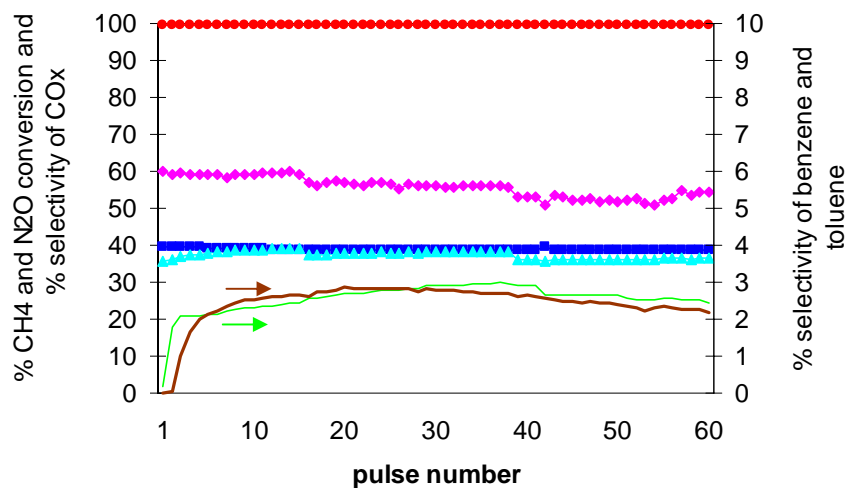
	Samples	$\chi_{CH_4}$	$S_{Ar}^a$	$Y_{Ar}^a$	Formation Rate <sup>a</sup> ( $\mu\text{mol/s.gcat}$ )		Deactivation time <sup>b</sup> (min)
					Benzene	Toluene	
No steam	Ex-Fe/SH27	22.0	22.1	4.86	0.54	4.29	6.26
	Ex-Fe/SH55	20.3	16.2	3.29	0.74	4.75	3.63
	Ex-V/SH27	24.9	20.2	5.03	0.86	4.60	5.53
	Ex-V/SH55	26.5	16.8	4.45	0.55	3.59	4.25
steam	Ex-Fe/SH27	21.7	20.5	4.45	0.95	7.02	9.23
	Ex-Fe/SH55	20.0	21.0	4.20	0.44	3.80	4.41
	Ex-V/SH27	24.5	17.5	4.29	0.60	4.78	8.40
	Ex-V/SH55	20.6	12.3	2.53	0.38	2.15	4.11

<sup>a</sup>data were recorded at maximum value

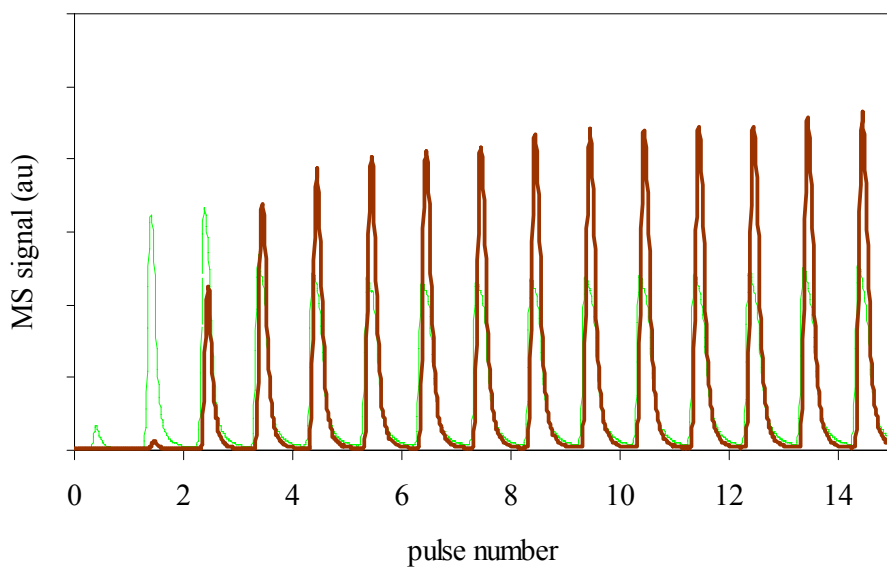
<sup>b</sup>deactivation time was time at a half of highest selectivity of aromatic

Table 8 showed that steamed and unsteamed samples had the same methane conversion about 20 % and the same selectivity for aromatic of about 20 %. The steam treatment enhanced the stability of the catalyst as seen from an increasing of deactivation time of all steamed samples. For example, the deactivation time of Ex-Fe/SH27 was 6.26 and after steam treatment the deactivation time was increased to 9.23. The coke formation selectivity reduced from 15 % to 10 % after steam treatment. The coke formation was significantly suppressed because the steam treatment reduced the Brønsted acid sites which coke was formed at these sites. Nevertheless, the catalysts were still suffered by the coke deposition and were deactivated within minutes of reaction.

## 2.5 Pulse Reaction



(a) Catalytic activity



(b) MS signal

**Figure 13** Pulse reaction on Ex-Fe/SH27 catalysts at 500 °C: (a) catalytic activity; %conversion of methane (■) and nitrous oxide (●); %selectivity of carbon monoxide (◆), carbon dioxide (▲), benzene (—), and toluene (—) (b) MS signal; signal of benzene (—) and toluene (—);

The catalytic performance of pulse reaction showed in Fig. 13(a). The nitrous oxide was completely converted, while the conversion methane was about 40 %. The major product of this reaction was carbon oxides, about 95 % selectivity. Benzene and toluene were observed at about 5 % selectivity. Although coke deposition caused by carbon accumulation on the acid sites can deactivate the catalysts, the coke formation in pulse reaction small occurred that showed the catalyst stability. Because the amount of product pulsed is small compared to the amount of catalyst and, therefore, the coking of the catalyst remained small.

Figure 13(b) shows the transient aromatics evolution. In the first pulse, only small amount benzene was formed. In the second pulse, the benzene formation increased about 10 times compared with the first pulse, and toluene began to form. After that benzene and toluene formation rates were increased and reach stable levels in subsequent pulses. These results suggested that benzene was formed before the formation of toluene and toluene was formed by methylation of benzene with methane.

## CONCLUSIONS

Partial oxidation of methane on HZSM-5 zeolites using nitrous oxide as an oxidant at low temperature (500 °C) was studied and found that carbon oxides were the major products and small amount of benzene and toluene were also observed. The catalysts were rapidly deactivated by coke deposited. The transition metals loaded on HZSM-5 improved the catalytic activity for the formation of benzene and toluene and reduced coke formation on catalysts. The formation rate of toluene of all catalysts was higher than that of benzene. At the ratio of  $\text{CH}_4/\text{N}_2\text{O} = 2$  and low Si/Al ratio gave the highest aromatic selectivity and the benzene and toluene formation. After steam treatment the conversion of methane and the selectivity of aromatics were unchanged, but the stability of these catalysts was slightly increased. However, catalysts still suffered from coke formation. The pulse reaction showed that benzene was formed before the toluene formation and aromatic formation increased with the number of pulse while only a small amount coke deposited was occurred.

## LITERATURE CITED

- Adebajo, M.O., M.A. Long and R.L. Forst. 2004. Further evidence for the oxidative methylation of benzene with methane over zeolite catalysts. **Catal. Commun.** 5: 125-130
- Cellier, C., D.L. Clef, C.M. Pedrero and P. Ruiz. 2005. Influence of the co-feeding of CO, H<sub>2</sub>, CO<sub>2</sub> or H<sub>2</sub>O in the partial oxidation of methane over Ni and Rh supported catalysts. **Catal. Today** 106: 47-57
- Chen, H.Y., S. Tang, Z.Y. Zhong, J. Lin and K.L. Tan. 2001. XPS and FTIR studied of Mo/HZSM-5 catalysts for nonoxidative conversion of methane to aromatics. **Surf. Rev. and Lett.** 8: 627-632
- Chen, L., L. Lin, Z. Xu, X. Li and T. Zhang. 1995. Dehydro-oligomerization of methane to ethylene and aromatics over Molybdenum/HZSM-5 catalyst. **J. Catal.** 157: 190-200
- Dimitrova, R., Y. Neinska, M. Mihályi, G. Pal-Borbély, M. Spassova. 2004. Reductive solid-state ion exchange as a way to vanadium introduction in BZSM and BBeta zeolites. **Appl Catal A** 266: 123-127
- Ding, W., S. Li, G.D. Meitzner and E. Iglesia. 2001. Methane conversion to aromatics on Mo/H-ZSM5: Structure of molybdenum species in working catalysts. **J. Phys. Chem. B** 105: 506-513
- Groen, J.C., L. Peffer and J. Perez-Ramirez. 2003. Pore size determination in modified micro- and mesoporous materials. Pitfalls and limitations in gas adsorption data analysis. **Micropor. Mesopor. Mater.** 60: 1-17
- Ha, V.T.T., L.V. Tiep, P. Meriaudeau and C. Naccache. 2002. Aromatization of methane over zeolite supported molybdenum: active sites and reaction mechanism. **J. Mol. Catal. A** 181: 283-290

- Kim, Y.H. and H.I. Lee. 1999. Redox property of vanadium oxide and its behavior in catalytic oxidation. **Bull. Korean Chem. Soc.** 20: 1457-1463
- Knops-Gerrits, P.P. and W.A. Goddard. 2001. Methane partial oxidation in iron zeolites: theory versus experiment. **J. Mol. Catal. A** 166:135-145
- Liu, H., T. Li, W. Shen, X. Bao and Y. Xu. 2004. Methane dehydroaromatization over Mo/HZSM-5 catalysts in the absence of oxygen: effects of silanation in HZSM-5 zeolite. **Catal. Today** 93-95: 65-73
- \_\_\_\_\_, \_\_\_\_\_, B. Tain and Y. Xu. 2001. Study of the carbonaceous deposits formed on a Mo/HZSM-5 catalyst in methane dehydro-aromatization by using TG and temperature-programmed techniques. **Appl. Catal. A** 213: 103-112
- Liu, W., Y. Xu, S. Wong, L. Wang, J. Qiu and N. Yang. 1997. Methane dehydrogenation and aromatization in the absence of oxygen on Mo/HZSM-5: A study on the interaction between MO species and HZSM-5 by using  $^{27}\text{Al}$  and  $^{29}\text{Si}$  MAS NMR. **J. Mol. Catal. A** 120: 257-265
- \_\_\_\_\_ and \_\_\_\_\_. 1999. Methane dehydrogenation and aromatization over Mo/HZSM-5: In situ FT-IR characterization of its acidity and the interaction between Mo species and HZSM-5. **J. Catal.** 185: 386-392.
- \_\_\_\_\_, S.Y. Yu, G.D. Meitzner and E. Iglesia. 2001. Structure and properties of Cobalt-Exchanged HZSM-5 catalysts for dehydrogenation and dehydrocyclization of alkanes. **J. Phys. Chem. B** 105: 1176-1184
- Liu, S., R. Ohnishi and M. Ichikawa. 2003. Promotional role of water added to methane feed on catalytic performance in the methane dehydroaromatization reaction on Mo/HZSM-5 catalyst. **J. Catal.** 220: 57-65

- Lobree, L.J., I. Hwang, J.A. Reimer and A.T. Bell. 1999. Investigations of the state of Fe in H-ZSM-5. **J. Catal.** 186: 242-253
- Lucas, A.D., J.L. Valverde, L. Rodriguez, P. Sanchez and M.T. Garcia. 2000. Partial oxidation of methane to formaldehyde over Mo/HZSM-5 catalysts. **Appl Catal A** 203: 81-90
- Lunsford, J. H. 2000. Catalytic conversion of methane to more useful chemicals and fuels: a challenge for the 21<sup>st</sup> century. **Catal. Today** 63: 165-174
- Ma, D., Y. Shu, X. Bao and Y. Xu. 2000. Methane Dehydro-aromatization under nonoxidative conditions over Mo/HZSM-5 catalysts: EPR Study of the Mo species on/in the HZSM-5 zeolite. **J. Catal.** 189: 314–325
- Ma, H., R. Kojima, R. Ohnishi and M. Ichikawa. 2004. Efficient regeneration of Mo/HZSM-5 catalyst by using air with NO in methane dehydro-aromatization reaction. **Appl. Catal. A** 275: 183–187
- \_\_\_\_\_, R. Ohnishi and M. Ichikawa. 2003. Highly stable performance of methane dehydroaromatization on Mo/HZSM-5 catalyst with a small amount of H<sub>2</sub> addition into methane feed. **Catal. Lett.** 89: 143-146
- Miao, S., L. Liu, Y. Lian, X. Zhu, S. Zhou, Y. Wang and X. Bao. 2004. On the reactivity of Mo species for methane partial oxidation on Mo/HMCM-22 catalysts. **Catal. Lett.** 97: 209-215
- Ohnishi, R., S. Liu, Q. Dong, L. Wang and M. Ichikawa. 1999. Catalytic dehydrocondensation of methane with CO and CO<sub>2</sub> toward benzene and naphthalene on Mo/HZSM-5 and Fe/Co-modified Mo/HZSM-5. **J. Catal.** 182: 92–103



Petras, M. and B. Wichterlova. 1992. High temperature interaction of vanadium pentoxide with H-ZSM-5 zeolite. ESR and IR study. **J. Phys. Chem.** 96: 805-1809

Shepelev, S.S. and K.G. Ione. 1983. Catalytic properties of zeolites with various structures and chemical composition in the preparation of aromatic hydrocarbons from methane. **React. Kinet. Catal. Lett.** 23: 319-322

\_\_\_\_\_ and \_\_\_\_\_. 1983. Preparation of aromatic hydrocarbons from methane in presence of oxygen. **React. Kinet. Catal. Lett.** 23: 323-325

Shu, Y. and M. Ichikawa. 2001. Catalytic dehydrocondensation of methane towards benzene and naphthalene over transition metal supported zeolite catalysts: templating role of zeolite micropores and characterization of active metallic sites. **Catal. Today** 71: 55-67

\_\_\_\_\_, R. Ohnishi and M. Ichikawa. 2003. Improved methane dehydrocondensation reaction on HMCM-22 and HZSM-5 supported rhenium and molybdenum catalysts. **Appl. Catal. A** 252: 315–329

Su, L., L. Liu, J. Zhuang, H. Wang, Y. Li, W. Shen, Y. Xu and X. Bao. 2003. Creating mesopores in ZSM-5 zeolite by alkali treatment: a new way to enhance the catalytic performance of methane dehydroaromatization on Mo/HZSM-5 catalysts. **Catal. Lett.** 92: 155-167

Tan, P.L., Y.L. Leung, S.Y. Lai and C.T. Au. 2002. Methane aromatization over 2wt% Mo/HZSM-5 in the presence of O<sub>2</sub> and NO. **Catal. Lett.** 78: 251-258

\_\_\_\_\_, \_\_\_\_\_, \_\_\_\_\_ and \_\_\_\_\_. 2002. The effect of calcinations temperature on the catalytic performance of 2wt% Mo/HZSM-5 in methane aromatization. **Appl. Catal. A** 228: 115-125

- Tan, P.L., K.W. Wong, C.T. Au and S.Y. Lai. 2003. Effect of Co-fed O<sub>2</sub> and CO<sub>2</sub> on the deactivation of Mo/HZSM-5 for methane aromatization. **Appl. Catal. A** 253: 305-316
- Tang, S., H. Chen, J. Lin and K.L. Tan. 2001. Non-oxidative conversion of methane to aromatics over modified Mo/HZSM-5 catalysts. **Catal. Commun.** 2: 31-35
- Wang, D., J.H. Lunsford and M.P. Rosynek. 1997. Characterization of a Mo/ZSM-5 catalyst for the conversion of ethane to benzene. **J. Catal.** 169: 347-358
- Wang, H., L. Su, J. Zhuang, D. Tan, Y. Xu and X. Bao. 2003. Post-steam-treatment of Mo/HZSM-5 catalysts: An alternative and effective approach for enhancing their catalytic performances of methane dehydroaromatization. **J. Phys. Chem. B** 107: 12964-12972
- Weckhuysen, B.M., D. Wang, M.P. Rosynek and J.H. Lunsford. 1998. Conversion of methane to benzene over transition metal ion ZSM-5 Zeolites: I. Catalytic characterization. **J. Catal.** 175: 338-346.
- \_\_\_\_\_, \_\_\_\_\_, \_\_\_\_\_ and \_\_\_\_\_. 1998. Conversion of methane to benzene over transition metal ion ZSM-5 Zeolites. II. Catalyst characterization by X-Ray Photoelectron Spectroscopy. **J. Catal.** 175: 347-351
- Xu, Y., X. Bao and L. Lin. 2003. Direct conversion of methane under nonoxidative conditions. **J. Catal.** 216: 386-395
- Zhang, C., S. Li, Y. Yuana, W. Zhang, T. Wu and L. Lin. 1998. Aromatization of methane in the absence of oxygen over Mo-based catalysts supported on different types of zeolites. **Catal. Lett.** 56: 207-213

Zhang, J.Z., M.A. Long and R.F. Howe. 1998. Molybdenum ZSM-5 zeolite catalysts for the conversion of methane to benzene. **Catal. Today** 44: 293-300

Zhang, S.G., S. Higgashimoto, H. Yamashita and M. Anpo. 1998. Characterization of vanadium oxide/ZSM-5 zeolite catalysts prepared by the Solid-State reaction and Their Photocatalytic Reactivity: In situ Photoluminescence, XAFS, ESR, FT-IR, and UV-vis Investigations. **J. Phys. Chem. B** 102: 5590-5594

## **APPENDIX**

## **Appendix A**

### **Calibration Method and Calculation method**

## Appendix A

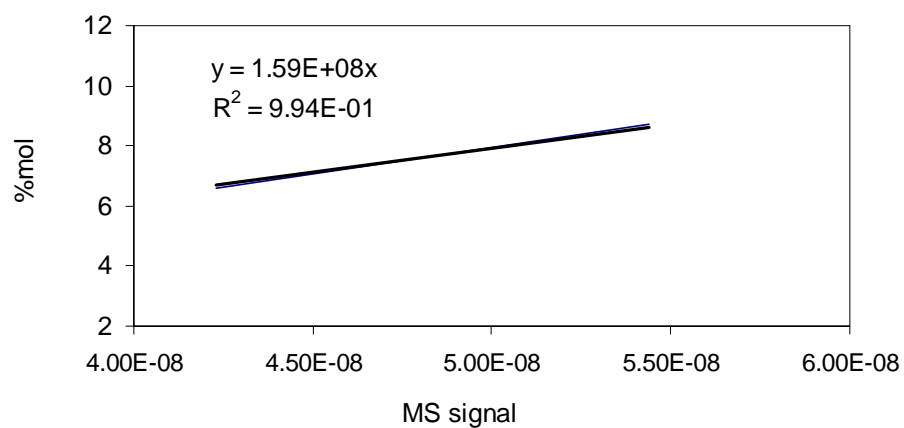
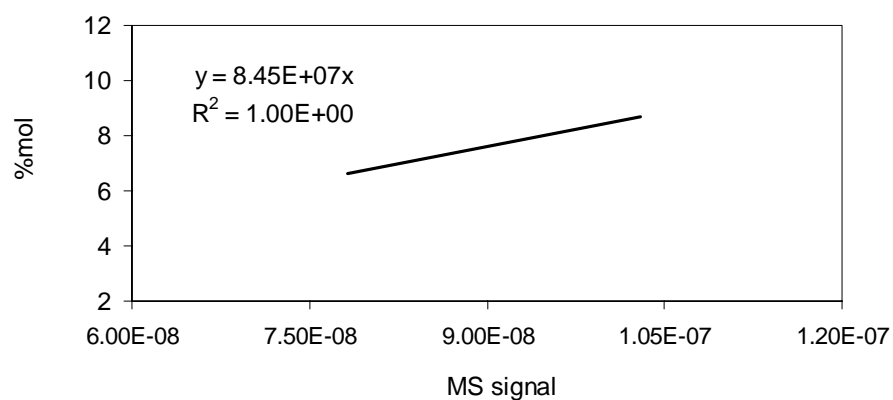
### **Calibration Method and Calculation method**

#### **1. Calibration Method**

Calibration of each gas was performed by measuring ion current or peak areas at various concentrations of each component by using the Quadrupole Mass spectrometer (Quardstar QMS422).

The fixed flow rates of CH<sub>4</sub>, CO, N<sub>2</sub>O, Ar, and CO<sub>2</sub> were diluted by various flow rate of He gas into three concentrations at room temperature. The mass fragments of chosen gases were m/e = 15 for CH<sub>4</sub>, m/e = 28 for CO, m/e = 28, 30 and 44 for N<sub>2</sub>O, m/e = 40 for Ar, and m/e = 44 for CO<sub>2</sub>. Calibration curves of each gas were plotted between molar percentages (%mol) versus ion current of gases.

The solution of 0.2%v/v benzene in toluene and 0.2%v/v toluene in benzene were prepared for calibration. The amount of 0.4 µl and 1.0 µl of aromatic mixture were injected by micro syringe into a heated inlet line with He flow rate = 50 ml/min as carrier gas at 100 °C. The mass fragments of chosen aromatics were m/e=78 of C<sub>6</sub>H<sub>6</sub> and m/e=91 of C<sub>7</sub>H<sub>8</sub>. The concentrations and the average of peak areas of aromatics were used to plot the calibration curve of aromatics.

(a) CH<sub>4</sub>

(b) Ar

**Appendix Figure A1** Calibration curves of (a) CH<sub>4</sub> and (b) Ar

The calibration curves were linear and the slopes of the linearity calibration curves defined the sensitivity of each component.

## 2. Calculation Method

The concentration (molar percentage) of each component in product can be calculated from relative response factor. Relative response factor is calculated from equation 1 based on the sensitivity of Ar that is the external standard.

$$\text{Relative response factor of gases} = \frac{\text{Sensitivity of gases}}{\text{Sensitivity of Ar}} \quad 1$$

**Appendix Table A1** Summarized of relative response factor of gases.

Gas	Relative response factor (RRF)
CO	0.602
CH <sub>4</sub>	1.882
N <sub>2</sub>	0.989
N <sub>2</sub> O(at m/e=44)	0.821
N <sub>2</sub> O(at m/e=30)	5.925
N <sub>2</sub> O(at m/e=28)	15.978
CO <sub>2</sub>	0.733
Benzene (B)	0.373
Toluene (T)	0.285
Ar	1

Determining the concentration of each component can be calculated by using equation 2:

$$\%mol \text{ of gases} = I_g \times S_{Ar} \times RRF_g \quad 2$$

Where  $I_g$  is ion current of gas component,  $S_{Ar}$  refers to sensitivity of argon gas, and  $RRF_g$  means relative response factor of each component based on argon



Calculated molar percentage (%mol) of each component as follows:

$$\%mol \text{ of } CH_4 = I_{CH_4} \times S_{Ar} \times RRF_{CH_4}$$

$$\%mol \text{ of } B \text{ or } T = I_{B/T} \times S_{Ar} \times RRF_{(B \text{ or } T)}$$

$$\%mol \text{ of } N_2O = I_{N_2O} \times S_{Ar} \times RRF_{N_2O \text{ at } m/e=30}$$

%mol of  $N_2$  is %mol of  $N_2O$  consumed

$$I_{N_2O \text{ at } m/e=44} = \frac{(\%mol \text{ } N_2O_{\text{at } m/e=44}) \times S_{Ar}}{RRF_{N_2O \text{ at } m/e=44}}$$

$$I_{CO_2} = I_{N_2O \text{ at } m/e=44} - I_{N_2O \text{ at } m/e=44}$$

$$\%mol \text{ of } CO_2 = I_{CO_2} \times S_{Ar} \times RRF_{CO_2}$$

$$I_{CO} = \text{signal of } 28 - I_{N_2} - (I_{N_2O \text{ at } m/e=44} \times \%N_2O_{\text{at } m/e=28}/100) - (I_{CO_2} \times \%CO_{2 \text{ at } m/e=28}/100) - \text{baseline at } 28$$

Where % $N_2O$  at  $m/e=28$  = 12%, and % $CO_2$  at  $m/e=28$  = 13%

$$\%mol \text{ of } CO = I_{CO} \times S_{Ar} \times RRF_{CO}$$

## **Appendix B**

### **Oral Presentation**

## Appendix B

### Oral Presentation

31<sup>th</sup> Congress on Science and Technology of Thailand 2005

18-20 October 2005 at Technology Suranaree University of Technology, Nakhon Ratchasima

**การศึกษาปฏิกิริยา Partial oxidation ของมีเทนบนโลหะทรานซิชันบน HZSM-5**

**Partial oxidation of methane on transition metals supported on HZSM-5 zeolites**

วายุณ วงศ์ไพบุญวัฒน์<sup>1</sup>, พิบูลย์ พันธุ์<sup>1,2\*</sup>

Wayoon Wongpaiboonwatana<sup>1</sup>, Piboon Pantu<sup>1,2\*</sup>

<sup>1</sup>Laboratory for Computational & Applied Chemistry, Chemistry Department, Kasetsart University, Bangkok 10900, Thailand

<sup>2</sup>Center of Nanotechnology, Kasetsart University, Bangkok 10900, Thailand

**บทคัดย่อ:** ศึกษาปฏิกิริยา partial oxidation ของมีเทน ด้วยตัวเร่งปฏิกิริยาที่มีโลหะทรานซิชัน (เหล็ก, โมลิบดีนัม, โคบอลต์ และ วานาเดียม) บน HZSM-5 zeolites โดยใช้ไนตรัสออกไซด์เป็นตัวออกซิไดส์ ที่อุณหภูมิค่าในช่วง 450-500°C พบว่า conversion ของมีเทนและไนตรัสออกไซด์เพิ่มขึ้นเมื่ออุณหภูมิเพิ่มขึ้น โดยในช่วงแรกของปฏิกิริยาจะเกิดเบนซินและโทลูอิน แต่ผลิตภัณฑ์ส่วนใหญ่จะเป็นคาร์บอนไดออกไซด์และคาร์บอนมอนอกไซด์ เมื่อเติมไฮโดรเจนในสารตั้งต้น จะทำให้ selectivity ของเบนซินและโทลูอินเพิ่มขึ้น และพบว่าMo/HZSM-5ให้ปริมาณเบนซินและโทลูอินสูงสุด

## Abstract

The activity and selectivity of the partial oxidation of methane over transition metals (Fe, Mo, Co and V) supported on HZSM-5 zeolites has been investigated using nitrous oxide as oxidizing agent at low temperature in the ranging from 450-500 °C. Methane and nitrous oxide conversion increased with the temperature. At the initial, benzene and toluene formation was observed. However, the main products were carbon dioxide and carbon monoxide. Addition of H<sub>2</sub> increased the selectivity of benzene and toluene. The Mo/HZSM-5 gave the highest selectivity to benzene and toluene.

## 1. Introduction

Conversion of methane to partial oxidized products, or higher hydrocarbons and aromatics has received great attention due to a strong economic incentive for better utilization of the abundant natural gas reserves worldwide. A number of strategies are explored and developed for the conversion of methane. There can be divided into two groups. The first is the direct method, synthesis of methanol and formaldehyde, oxidative coupling and conversion of methane to aromatic. Indirect conversion is the production of synthesis gas, synthesis of methanol, and Fischer-Tropsch synthesis.

### 1.1 Direct Conversion of Methane

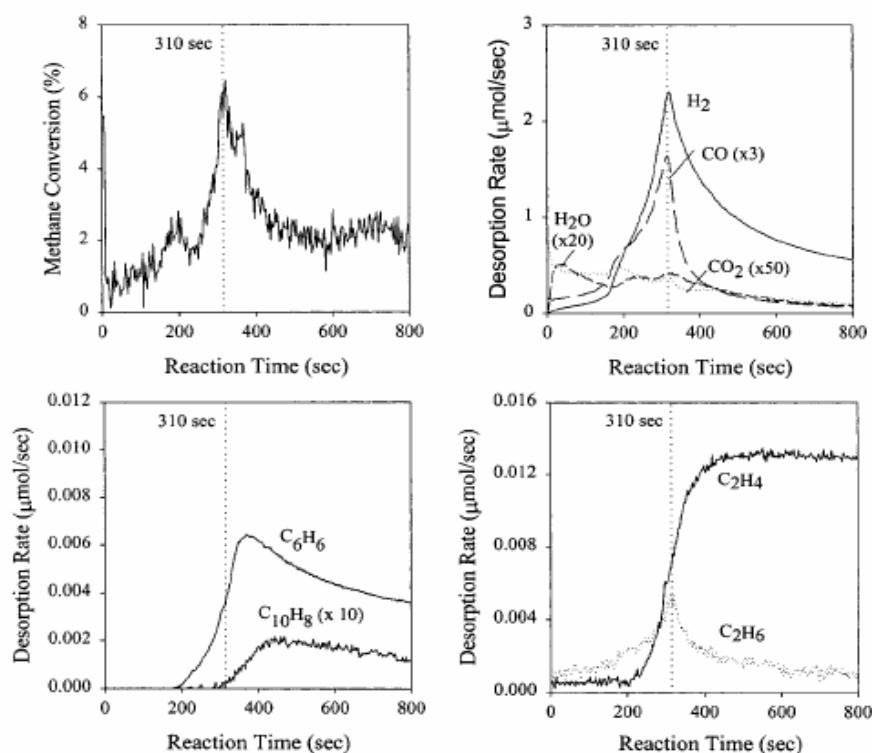
Y. Xu et al. (2003), methane dehydroaromatization (MDA) is the most interesting in the direct conversion of methane. The generally use Mo/HZSM-5 for MDA because:

- Mo/HZSM-5 is a bifunctional catalyst
- There require an induction period to reduce MoO<sub>x</sub> to Mo<sub>2</sub>C and/or MoO<sub>x</sub>C<sub>y</sub> species before production of aromatics.
- The molecular shape selectivity of the zeolite channels will remarkably affect the product distribution of the reaction. (Silica–alumina-type zeolites with a

two-dimensional structure and a pore size near the dynamic diameter of benzene (0.59 nm) are good supports of the Mo-based catalysts for MDA.)

- But heavy carbonaceous deposits are formed during the reaction and lead to deactivation of the Mo/HZSM-5 catalysts.

## 1.2 Induction period



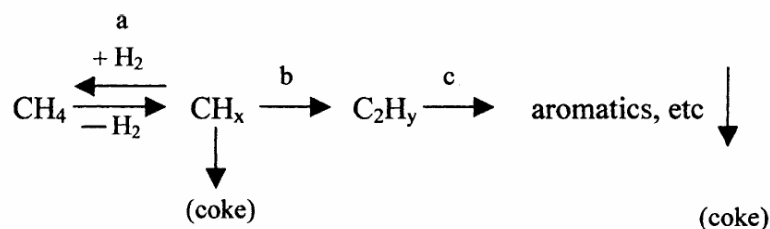
**Appendix Figure B1** Transient reaction of 4 wt % Mo/H-ZSM5 with methane.  
(Ding et al., 2001)

Fig. B1 shows reaction profiles of methane dehydroaromatization. In the initial of the reaction about 300s, methane conversion is low and no production of benzene and C2 HCs, but lead to  $CO_2$ ,  $H_2O$ ,  $H_2$  and  $CO$  without the formation of hydrocarbons. This calls induction period. After the induction period, conversion of methane increased sharply and subsequently decreased and formation of benzene and C2. The quantity of  $H_2$  was more than two times larger than that of C; this shows that

some carbon was retained by the catalyst as carbidic carbon, carbon containing reactive intermediates, or deactivating deposits.

### 1.3 Bifunctional Mechanism

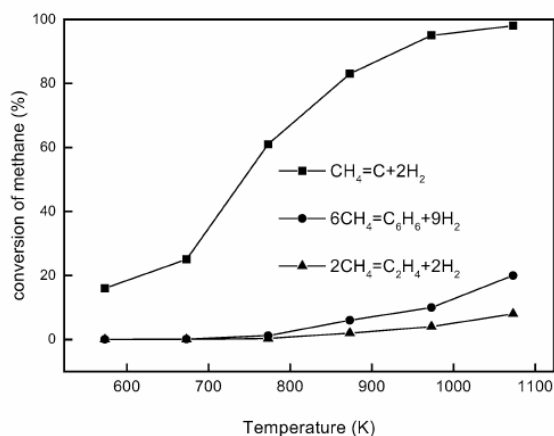
From previous results suggest that Mo(VI) species were reduced during the induction period and converted to  $\text{MoC}_x$  or  $\text{MoO}_x\text{C}_y$  and active for  $\text{C}_2$  formation as the primary intermediates, while the acidic sites on HZSM-5 catalyze the subsequent conversion of benzene as following with Fig. B2 (Y. Shu et al, 2001).



#### Appendix Figure B2 Bifunctional Mechanism

Where: a, b are on a Mo site of carbide or oxycarbide, and c is on HZSM-5

### 1.4 Thermodynamic limit



**Appendix Figure B3** Thermodynamic limit of direct conversion of  $\text{CH}_4$  under nonoxidative conditions. Y. Xu et al. (2003)

Due to the strong C-H bonds, its high chemical stability of methane, direct conversion of methane to useful chemicals is still limited by low conversion of methane and/or low selectivity. Fig. B3 shows the thermodynamics limit of direct conversion of methane under non oxidative condition. CH<sub>4</sub> decomposition to carbon and hydrogen increased with temperature. Therefore, methane conversion to carbon and hydrogen is easier than benzene and C<sub>2</sub> hydrocarbons. In general, MDA use temperature at 700°C, we found that the formation of coke easier than benzene and C<sub>2</sub>.

## **2. Propose addition oxidant**

The aromatization of methane in high reaction temperature is suffered by the high rate of coke formation. Therefore, the using of nitrous oxide as an oxidant in feed gas to relieve thermodynamic unfavorable, N<sub>2</sub>O in feed gas to gives oxygen anion radical on metal surface which is a reactive oxygen and may reduce temperature for activation at low temperature and to reduce coke formation.

## **3. Experimental Section**

### **3.1 Preparation of transition metal impregnated HZSM-5**

HZSM-5 zeolites supported transition metals were prepared by impregnation with the aqueous solution of Fe(NO<sub>3</sub>)<sub>3</sub>·9H<sub>2</sub>O, Co(NO<sub>3</sub>)<sub>2</sub>·6H<sub>2</sub>O, NH<sub>4</sub>VO<sub>3</sub> and (NH<sub>4</sub>)<sub>6</sub>Mo<sub>7</sub>O<sub>24</sub>·4H<sub>2</sub>O. The HZSM-5 zeolite powder will impregnate in a rotary evaporator at 80 °C with transition metal aqueous solution for 6h and then removed the water. The samples were dried overnight at 80 °C. The resulting catalysts were calcined in air at 550 °C for 5 hours and sieved to 40-60 mesh size.

### **3.2 Characterization of catalysts**

Temperature programmed reduction (TPR) was performed to the oxidation state of transition metals. The amount of powdered catalyst (0.1 g) was

pretreated by 10%O<sub>2</sub>/Ar (total flow 60 ml min<sup>-1</sup>) heating in at 550 °C (heating rate 10°C min<sup>-1</sup>) for 2 h then cooled to room temperature in Ar gas before starting the reaction. Flushing the samples with Hydrogen 2 % in Ar gas is used at a total flow rate of 30 ml/min and heating rate of 10 °C/min. The H<sub>2</sub> consuming has been detected by Mass spectrometer as detector.

### **3.3 Catalytic activity testing**

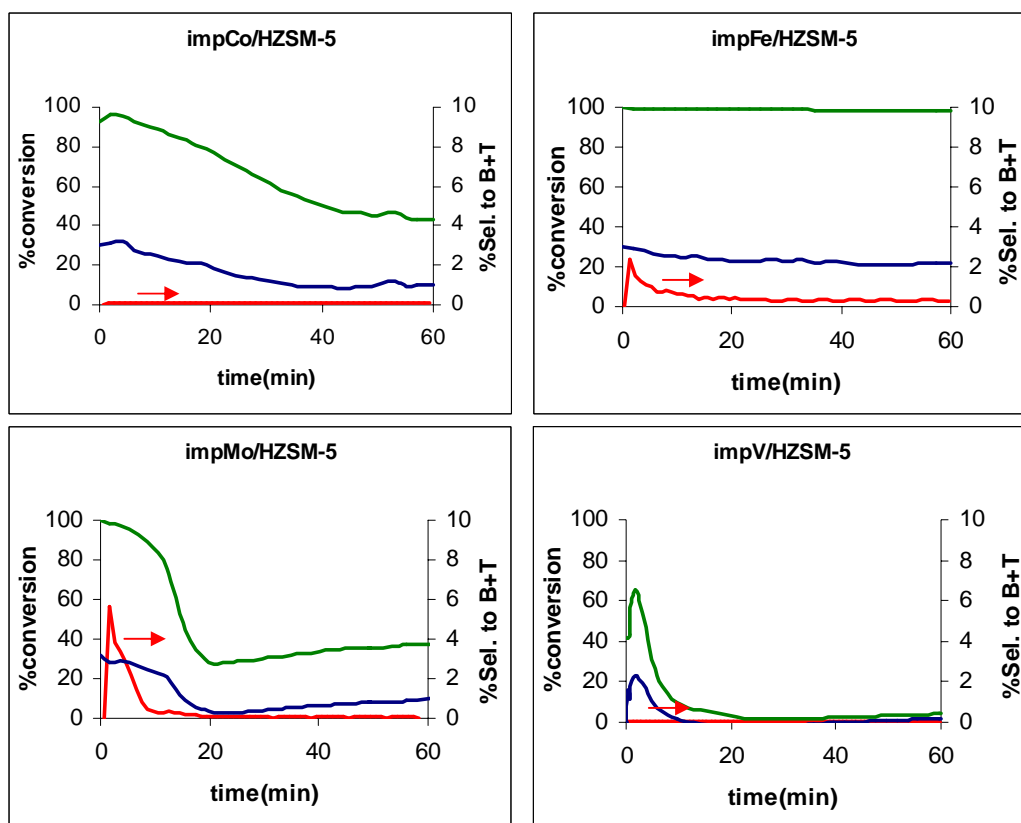
A fixed bed tubular reactor was used for catalytic activity testing. The quartz tube, 60 cm long and 0.43 cm i.d., was packed with glass wool to hold 0.05 g of the catalyst in place and covered with a layer of quartz beads to obtain a uniform gas distribution. The catalyst was heated under a 10%O<sub>2</sub>/He (60 ml/min) to 600 °C and maintained at 600 °C for 1h, and then a 10%H<sub>2</sub>/He (60ml/min) for 1h at 550 °C. The reaction gas is a mixture of CH<sub>4</sub>, N<sub>2</sub>O, H<sub>2</sub> and Ar (used as internal standard) and balance with He. The reaction condition using in the experiment were as follows: temperature, 450-500 °C; total flow rate, 100 ml/min; pressure, 1 atm; time on stream, 15 min. The products are analyzed by on-line gas chromatography with a column packing is Porapak Q and Hayesep D and TCD detector for the separation of gas products and Mass spectrometer for analyze the aromatic products.

## **4. Results and Discussion**

### **4.1 Catalytic performance of various catalysts at 450°C**

In the reaction carbon oxides was the major products. The formation of benzene and toluene was also observed. Among the four catalysts, the Co/HZSM-5 showed high conversion of methane and nitrous oxide but no selectivity to aromatics. The Fe/HZSM-5 had complete conversion of nitrous oxide and a rather stable conversion of methane but with small selectivity for aromatic. The V/HZSM-5 showed a very small selectivity of aromatic compounds. But the Mo/HZSM-5 is the best catalyst with the highest selectivity.



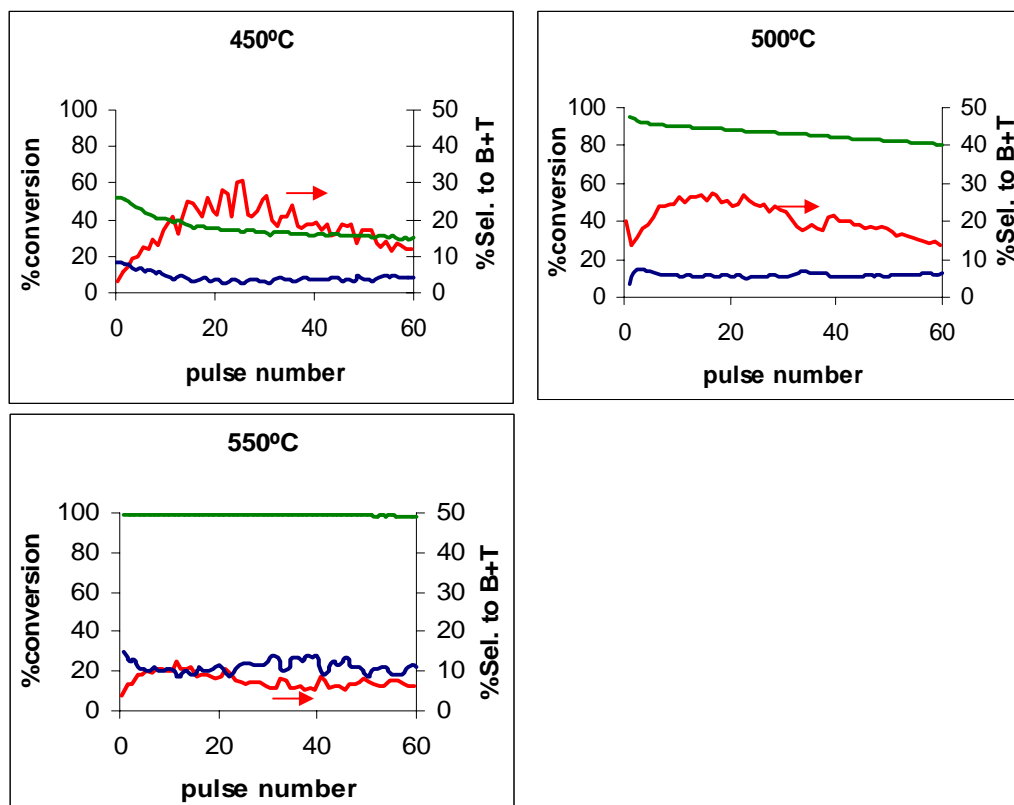


**Appendix Figure B4** Catalytic performance of various catalysts at 450 °C:

Conversion of methane (—); nitrous oxide (—); Formation of aromatic (—).

#### 4.1 Pulse Reaction

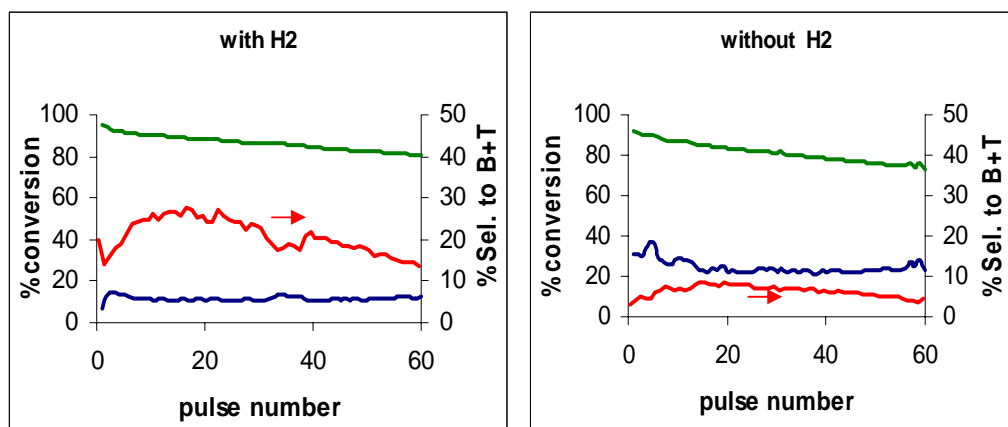
So we choose the Mo/HZSM-5 to study pulse reaction for observed transient behavior. We found that at 450 °C conversion of methane and N<sub>2</sub>O decreased but aromatic formation increased. When increase the temperature at 500 °C conversion of methane and N<sub>2</sub>O increased. And at 550 °C complete N<sub>2</sub>O conversion but lowest selectivity of aromatics. Therefore, 500 °C is the optimum temperature of this reaction.



**Appendix Figure B5** Pulse reaction on 2% wt Mo/HZSM-5 catalysts: Conversion of methane (—); nitrous oxide (—); Formation of aromatic (—).

#### 4.2 Effect of H<sub>2</sub> addition

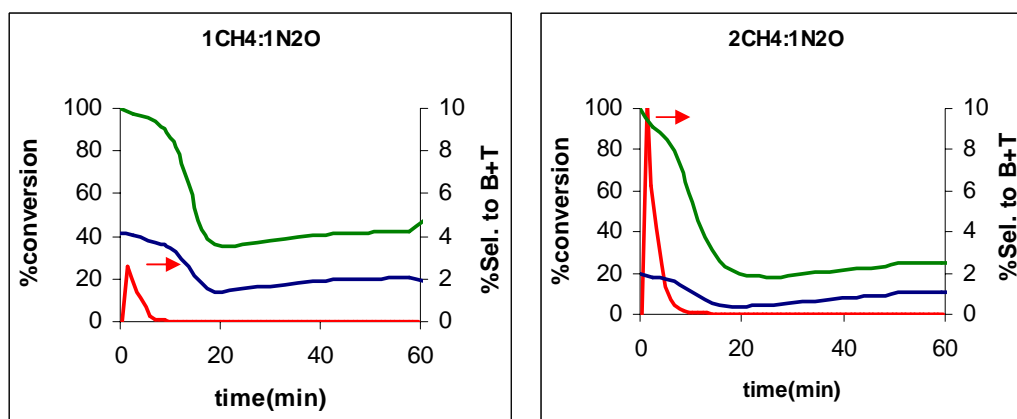
Figure B6 shows the effect of H<sub>2</sub> addition to pulse reaction on Mo/HZSM-5 catalyst. When add the H<sub>2</sub>, the conversion of methane decreased but the selectivity of aromatic increased because of thermodynamic limitation of MDA.



**Appendix Figure B6** Effect of H<sub>2</sub> addition to pulse reaction on 2% wt Mo/HZSM-5 catalysts with and without H<sub>2</sub> at 500 °C: Conversion of methane (—); nitrous oxide (—); Formation of aromatic (—).

#### 4.3 The effect of the ratio of CH<sub>4</sub> to N<sub>2</sub>O

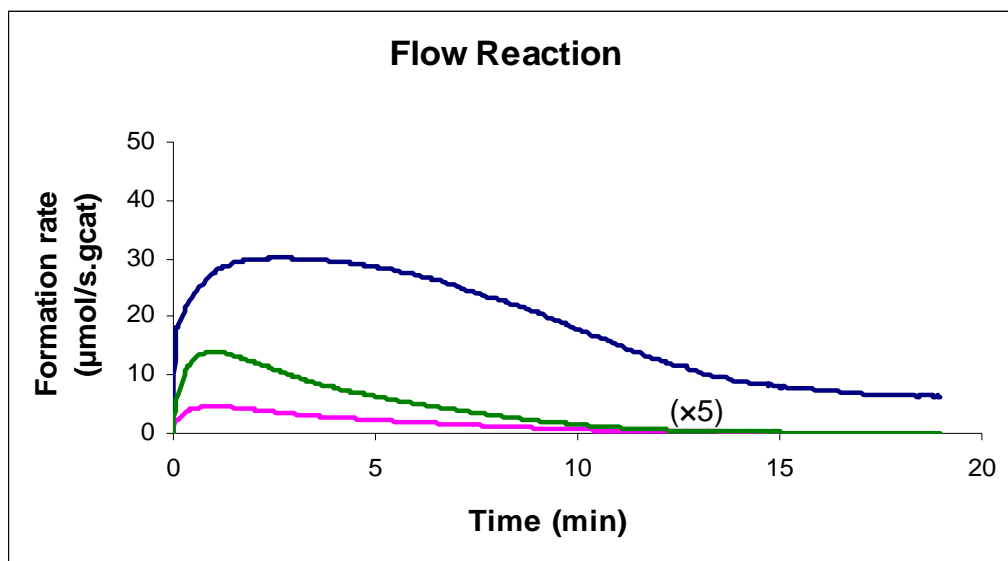
The ratio of CH<sub>4</sub>/N<sub>2</sub>O has the effect to catalytic activity. When we increase the ratio of CH<sub>4</sub>/N<sub>2</sub>O = 2, the maximum selectivity increased from 2% to 10%, while CH<sub>4</sub> and N<sub>2</sub>O conversion decreased faster than the low ratio. Because the coke deposited on catalyst at higher ratio occurred more than the low one as the following with figure B7.



**Appendix Figure B7** Effect of  $\text{CH}_4:\text{N}_2\text{O}$  ratio on 2% wt Mo/HZSM-5 catalysts without  $\text{H}_2$  at 500 °C;  $\text{CH}_4:\text{N}_2\text{O} = 1$  and  $\text{CH}_4:\text{N}_2\text{O} = 2$ :  
Conversion of methane ( ); nitrous oxide ( ); Formation of aromatic ( )

#### 4.4 Formation Rate of B and T

Figure B8 is the formation rate of benzene and toluene, toluene formation is higher than benzene formation. While it difference from the aromatic formation that was studied by other researchers. Such as in the Fig.B1, the benzene formation is higher than other aromatics and the mechanism of conversion of methane to aromatic also different from other researchers.



**Appendix Figure B8** Formation rate of benzene and toluene and  $\text{CH}_4$  conversion on 2% wt Mo/HZSM-5 catalysts at 500 °C: conversion of methane (—); Formation rate of benzene (—) and toluene (—).

#### 4.5 Propose Mechanism

From the previous results we can propose mechanism of this reaction. In first step,  $\text{N}_2\text{O}$  deposits of active species of  $\text{N}_2\text{O}$  on the metal surface, the second is the activation of methane to form methoxy radical that can occur at low temperature and coupling with  $\text{CH}_4$  to form  $\text{C}_2$  hydrocarbon.  $\text{C}_2$  can aromatize to benzene. Finally benzene reacts with methoxy radical to form toluene easily by acid sites on HZSM-5 zeolites.

1.  $\text{N}_2\text{O} + \text{MO}_x = \text{O}_x\text{M}[\text{O}] + \text{N}_2$
2.  $\text{O}_x\text{M}[\text{O}] + \text{CH}_4 = \text{O}_{x-1}\text{MOH}[\text{OCH}_3]$
3.  $\text{O}_{x-1}\text{MOH}[\text{OCH}_3] + \text{CH}_4 = \text{MO}_x + \text{C}_2\text{H}_y + \text{H}_2\text{O}$
4.  $3\text{C}_2\text{H}_y + \text{HZSM-5} = \text{C}_6\text{H}_6 + n\text{H}_2$
5.  $\text{C}_6\text{H}_6 + \text{O}_{x-1}\text{MOH}[\text{OCH}_3] = \text{MO}_x + \text{C}_6\text{H}_5\text{CH}_3 + \text{H}_2\text{O}$

## **5. Conclusion**

1. The using of nitrous oxide as an oxidant in feed gas give oxygen anion radical on metal surface to reduce methane activation temperature and relieve thermodynamic unfavorable and reduce coke formation.

2. The Mo supported HZSM-5 shows the highest activity for methane partial oxidation to higher hydrocarbon.

3. Addition of  $H_2$  in feed gas reduces methane conversion but increases benzene and toluene formation.

4. Formation rate of toluene is higher than benzene formation suggesting that these catalysts are active for methylation of benzene.

## **Acknowledgements**

Thank you for financial support from the Ministry of University Affairs under the Science and Technology Higher Education Development Project (MUA-ADB), Kasetsart University Research and Development Institute (KURDI) and Graduated School, Kasetsart University (Thesis and Dissertation Support Fund to W.W.)

## CURRICULUM VITAE

### PERSONAL DATA

Name: Miss Wayoon Wongpaiboonwatana  
 Date of birth: August 17, 1980  
 Place of birth: Nan, Thailand  
 Nationality: Thai

### EDUCATION

: YEAR	INSTITUTION	DEGREE
1998-2001	Chiangmai University	B.Sc. (Chemistry)

**SCHOLARSHIP :** Higher Education Development project  
 Scholarship Postgraduate Education and Research  
 Program in Physical Chemistry (2002-2003)

Graduated School, Kasetsart University (Thesis and  
 Dissertation Support Fund (2004-2005))

### PRESENTATION

Wayoon Wongpaiboonwatana and Piboon Pantu. **Partial Oxidation of Methane on Transition Metal supported on HZSM-5 (Oral)**. 31<sup>st</sup> Congress on Science and Technology of Thailand (STT 2005), 18-20 October 2005 at Technology Suranaree University of Technology, Nakhon Ratchasima.